PhD Thesis / Tesi Doctoral

INTRATHECAL ADMINISTRATION OF AAVrh10 CODING FOR β-GLUCURONIDASE CORRECTS BIOCHEMICAL AND HISTOLOGICAL HALLMARKS OF MUCOPOLYSACCHARIDOSIS TYPE VII MICE AND IMPROVES BEHAVIOR AND SURVIVAL

Author / Autora:

Director / Directora:

Gemma Pagès i Pi

Assumpció Bosch Merino

Doctorat en Bioquímica, Biologia Molecular i Biomedicina
Departament de Bioquímica i Biologia Molecular
Universitat Autònoma de Barcelona

2015

2.2.4 Histopathology

Besides the biochemical effects observed with the AAVrh10-GUSB treatment in MPS VII mice, we wanted to assess whether they correlated with histological changes in the same organs and tissues. Thus, representative peripheral organs and CNS and PNS samples from mice of each group and each time point were analyzed by microscopy. Wild type, and also heterozygote mice were used as controls, since the latter do not present any histological affectation.

Liver and heart were the somatic organs analyzed (**Figures 44** and **45** respectively).
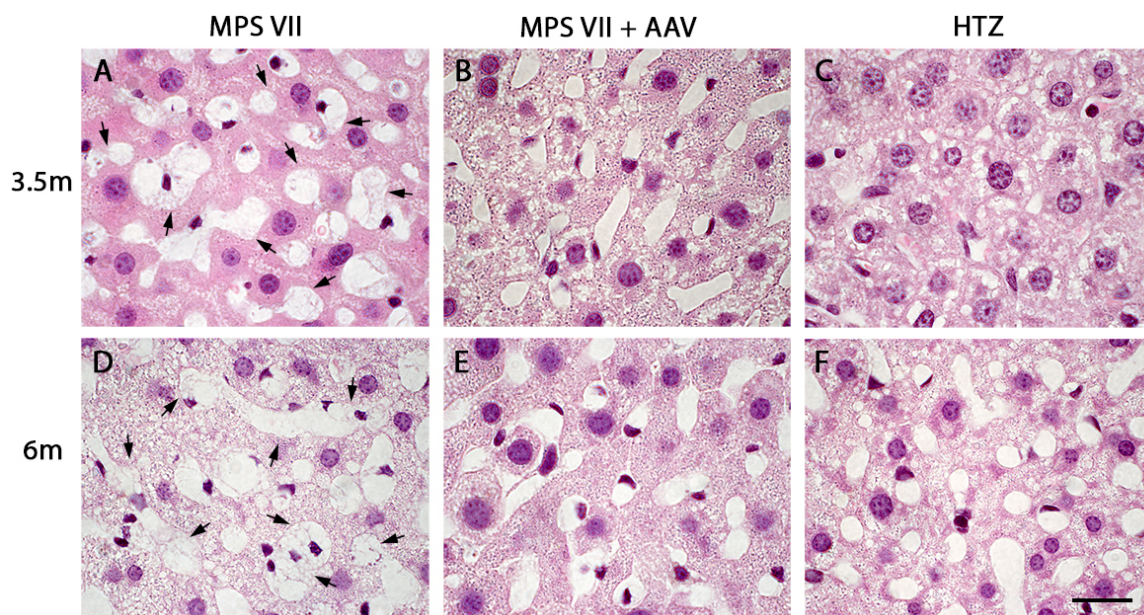

Figure 44: Liver histopathology. Staining: hematoxilin & eosin. Scale bar: 20 µm.
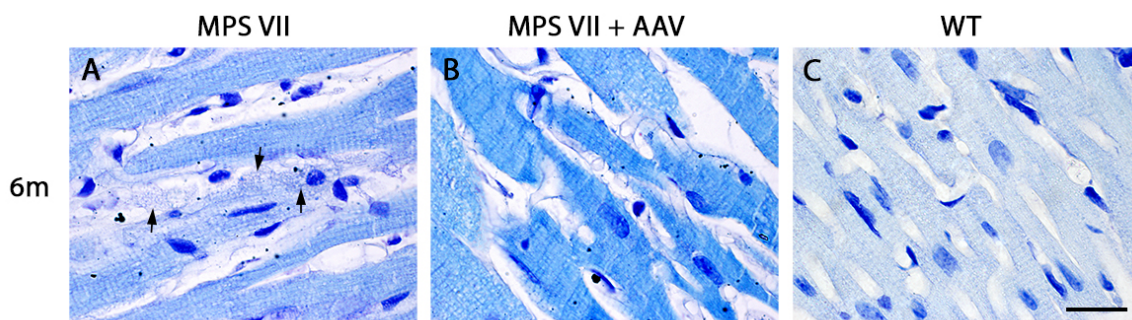

Figure 45: Cardiac muscle histopathology. Staining: toluidine blue. Scale bar: 20 µm

MPS VII mice of both ages present large vesicle accumulations throughout the hepatic tissue that are characteristic of the pathology (**Figure 44**). These accumulations are not present in any of the AAV-treated MPS VII mice.

Concerning heart, **Figure 45** shows cardiac muscle samples of 6-month-old mice (3.5-month-old samples were not available). In the myocardium, MPS VII mice present areas with abundant storage in the perivascular and interstitial cells and fewer large vacuoles in the myocytes. In contrast, AAV-treated MPS VII mice do not present these vesicle accumulations, looking more similar to WT mice. Therefore, treatment with AAVrh10-GUSB is able to correct the histological features of MPS VII mice in liver and cardiac muscle at 6 months of age.

The histological analysis of brain was done in cortex (**Figure 46**) and cerebellum (**Figure 47**), being two areas representative of high and low β-glucuronidase expression, respectively.
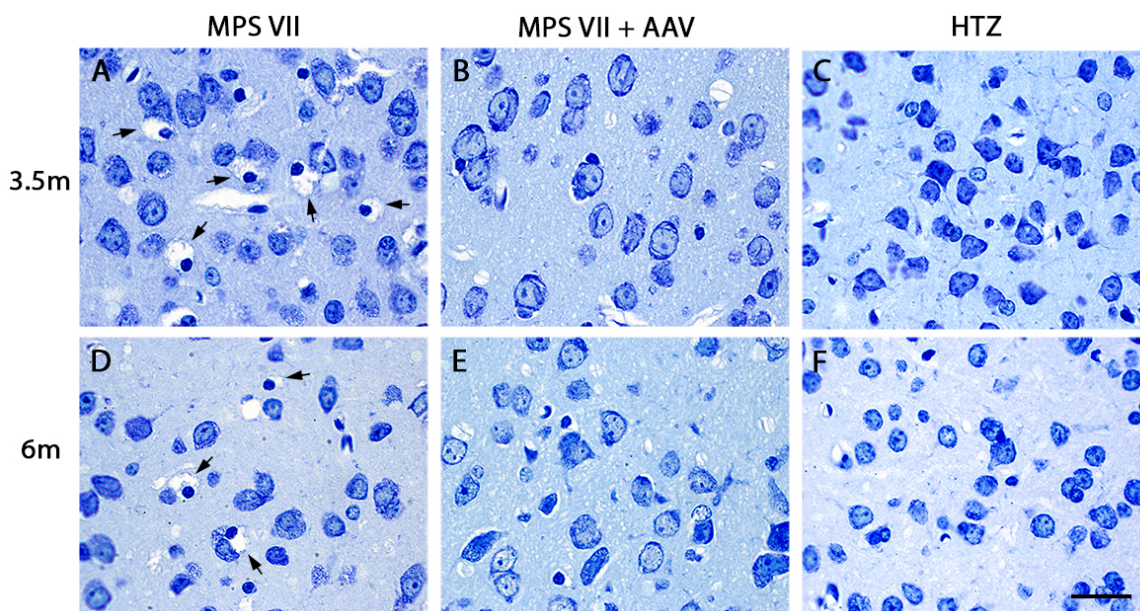

Figure 46: Cortex histopathology. Staining: toluidine blue. Scale bar: 20 μm.

In **Figure 46** it is evident that MPS VII cortices present vesicle accumulations at both ages analyzed. The most evident accumulations appear in the cytoplasm of neuroglial cells, which are identified by their small and dense nuclei and distributed among the neurons. Not as evident, accumulation of small vacuoles is also present in many neurons. In contrast, AAV-treated MPS VII mice cortices cytoplasm of the neuroglial cells is indistinguishable or very small, without vacuoles, resembling that of HTZ mice.
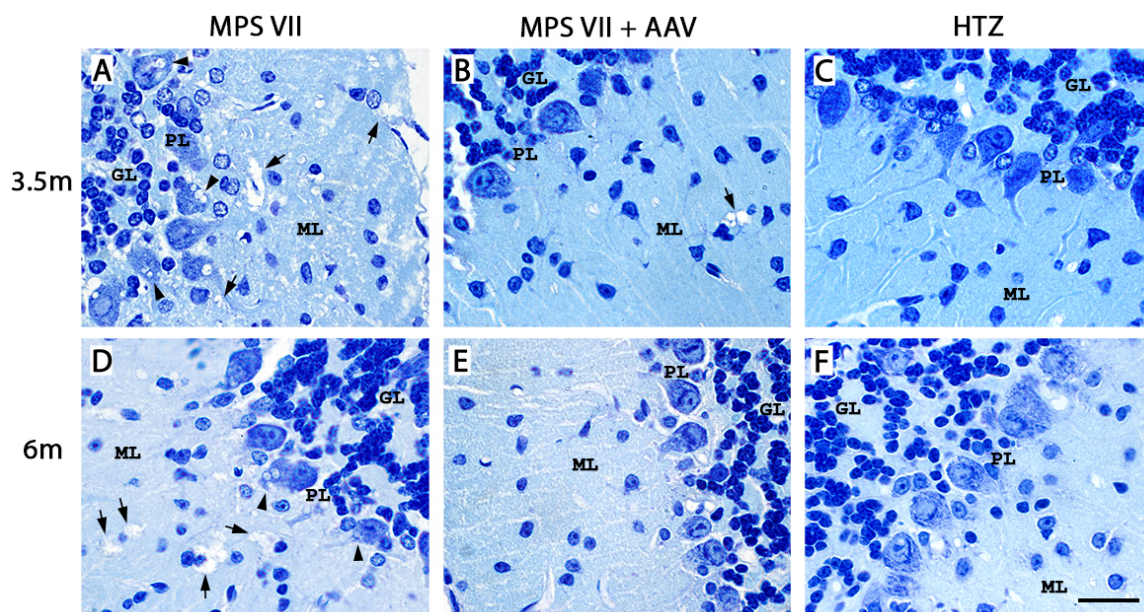

Figure 47: Cerebellum histopathology. GL, granular layer; PL, Purkinje layer; ML, molecular layer. Staining: toluidine blue. Scale bar: 20 μm.

Concerning cerebellum, **Figure 47** shows slices where the granular layer (GL), Purkinje layer (PL) and molecular layer (ML) can be distinguished. MPS VII mice present vesicle accumulations beside the nuclei of cells of the molecular layer and also into the cytoplasm of Purkinje neurons. The treatment with AAVrh10-GUSB is able to decrease the vesicle accumulation in the cerebellum, but not to correct it completely, since slices from AAV-treated mice of both ages still present some cells with vesicles. In order to quantify the number of cells presenting vesicle accumulations, we used samples from 3 MPS VII and 4 AAV-treated mice of 6 months of age. Quantification revealed that the treatment with AAVrh10-GUSB decreased the number of cells presenting vesicle accumulations to 20% of the MPS VII non-treated

mice. Therefore, brain transduction with AAVrh10-GUSB is able to correct the histological impairment in cortex and up to 80% in cerebellum. A possible explanation for this phenomenon is the low β-glucuronidase activity levels found in cerebellum of AAV-treated MPSVII mice, which do not reach WT levels, whereas in cortex they are higher than WT (see Figure 32).

Spinal cord and DRG samples were also assessed for vesicle accumulation (**Figure 48** and **49** respectively).
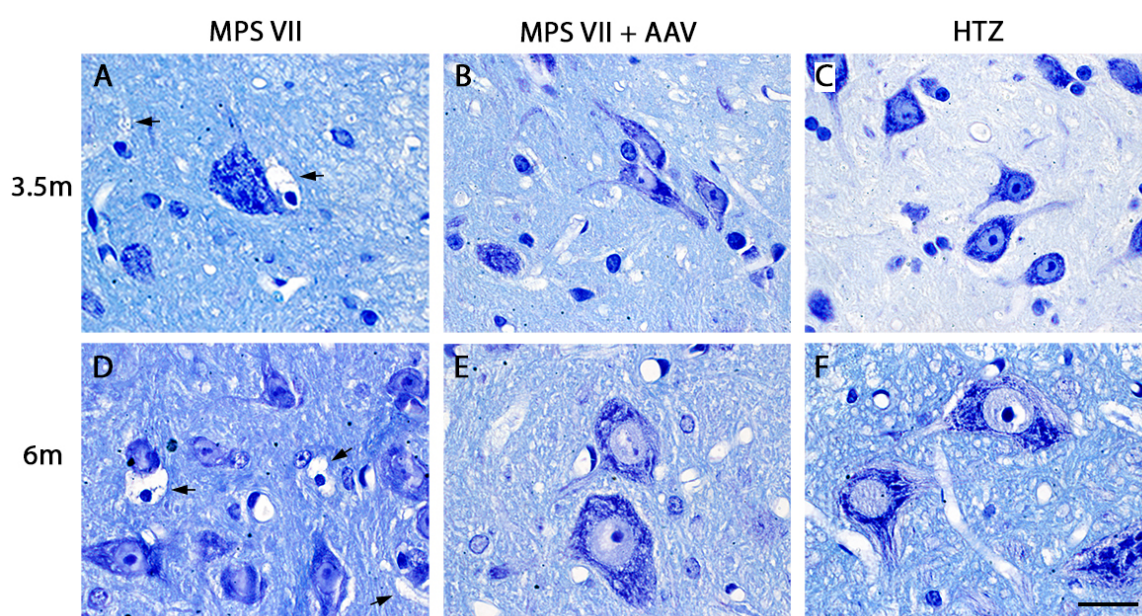

Figure 48: Spinal cord histopathology. Staining: toluidine blue. Scale bar: 20 μm.

Figure 48 depicts spinal cord samples showing a grey matter area with motor neurons. MPS VII mice present, as in cortex, vesicle accumulations surrounding neuroglial nuclei that are not seen in heterozygote mouse samples. These accumulations are scarcely seen in the AAV-treated MPS VII mice analyzed.
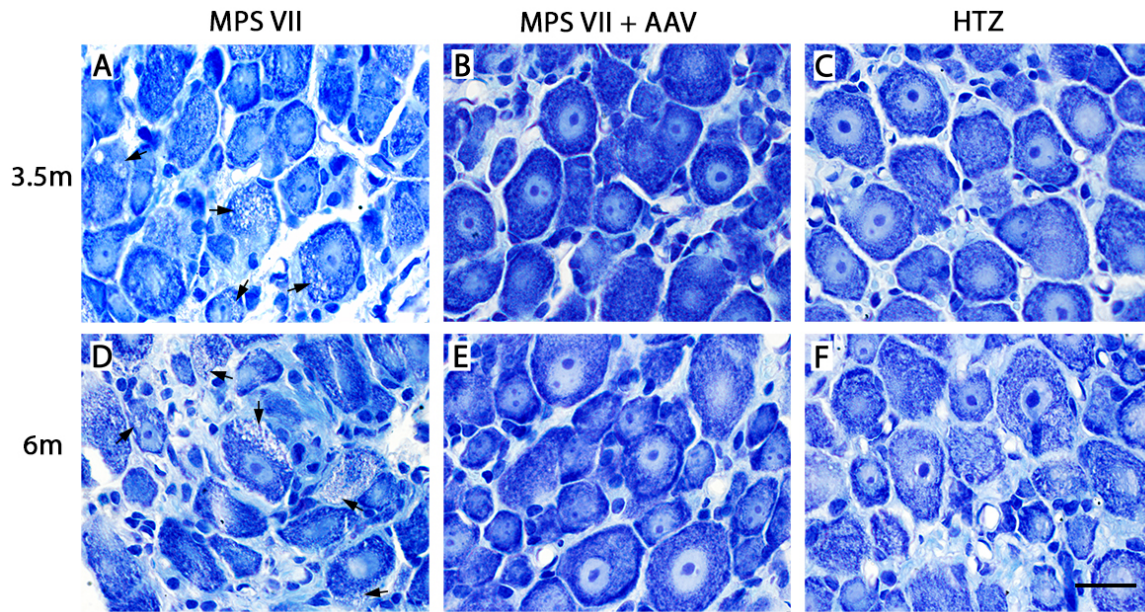
Figure 49: DRG histopathology. Staining: toluidine blue. Scale bar: 20 μm.

Finally, DRG samples are shown in **Figure 49**. MPS VII DRG present vesicle accumulations in the cytoplasm of sensory neurons, in contrast to heterozygote DRG samples. AAV treatment of MPS VII mice is able to eliminate these accumulations at both time points analyzed.

In conclusion, the intrathecal treatment with AAVrh10-GUSB is capable of substantially improving the histological feature of GAG vesicle accumulation of MPS VII mice in all the tissues analyzed, even at the shortest experimental time point.

2.2.5. ASTROGLIOSIS

Reactive astrogliosis is a marker of diseased CNS tissue present in many different CNS disorders and pathological situations (Sofroniew and Vinters (2009)). Concerning mucopolysaccharidosis, mild or moderate reactive astrogliosis has been described in MPS I, MPS IIIA, MPS IIIB mouse models (Wilkinson et al. (2012), Baldo et al. (2012)), as well as in MPS VII. In particular, an MPS VII mouse model exhibits increased GFAP staining in cortical and hippocampal regions (Heuer et al. (2002)), and whole transcriptome analysis of the brain of this model demonstrated increased expression of GFAP and other astrocyte cell-specific genes (Parente et al. (2012)).

Therefore, in this work we assessed reactive astrogliosis in the cortex by GFAP immunofluorescence (**Figure 50**) and by western blot (**Figure 51**).
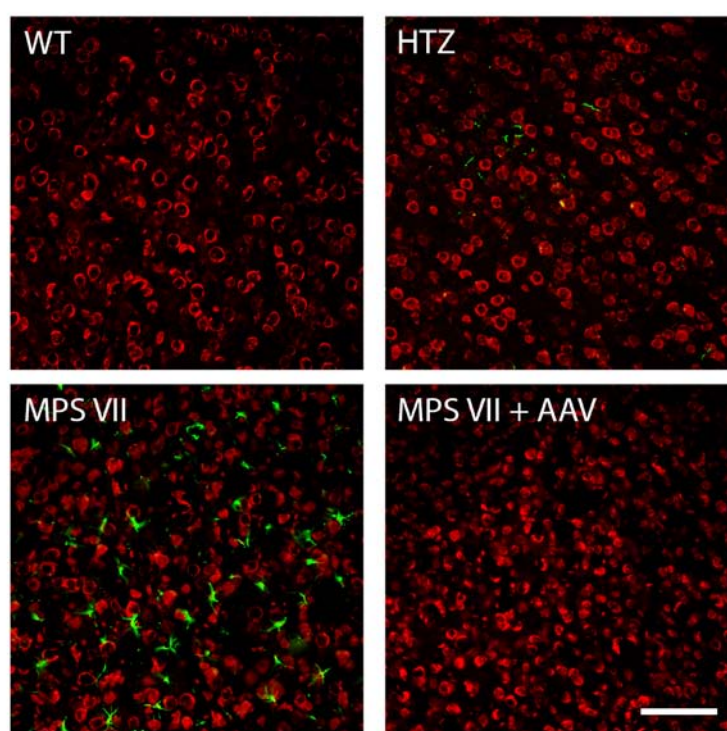
Figure 50: Astrogliosis in MPS VII cortex. Cortex stained with anti-GFAP (green) and counterstained with fluorescent Nissl stain (red). Scale bar: 100 μm.

Fluorescent histological GFAP staining of 6-month-old WT, HTZ, MPS VII and AAV-treated MPS VII mice reveal reactive astrogliosis in the cortex of MPS VII mice, and to a lesser extent in HTZ mice, whereas WT and AAV-treated MPSVII mice do not present any GFAP staining (**Figure 50**).
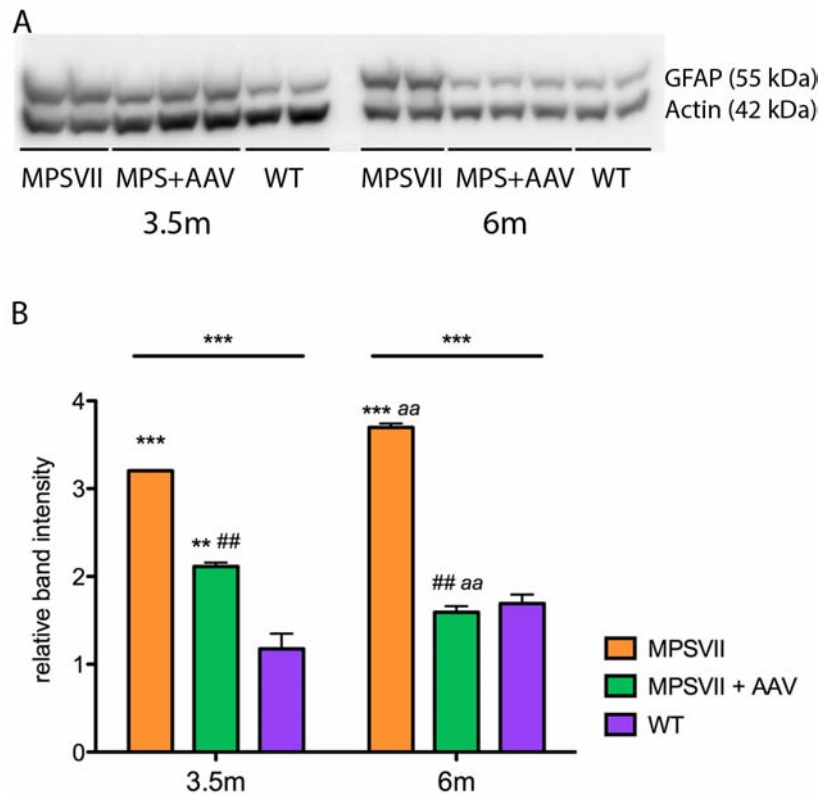
Figure 51: GFAP western blot of cortex samples. (**A**) GFAP western blot image. (**B**) Quantification of GFAP western blot. Sample size for each time point: n = 2 MPS VII; n = 3 MPS VII + AAV; n = 2 WT. Statistical analysis: Two-way ANOVA shows group effect ($p < 0.001$) at both ages and age effect in both MPS VII groups ($p < 0.01$). One-way ANOVA and Tukey *post hoc* analysis for each time point are depicted on the graph. *vs. WT; #vs. MPS VII; [a]age effect.

Figure 51 shows GFAP expression analysis by western blot in WT, MPS VII and AAV-treated MPS VII mice, at the two experimental time points. Correlating with the GFAP immunofluorescence analysis, MPS VII cortices present higher GFAP expression than WT at both ages. In addition, while GFAP does not vary with the age in WT mice, 6-month-old MPS VII mice present higher GFAP expression than 3.5-month-old mice, an age-related effect on reactive astrogliosis that is also described for MPS I, MPS IIIA and MPS IIIB (Wilkinson et al. (2012)). The AAV treatment in MPS VII mice is able to significantly lower GFAP expression in cortex at 3.5 months of age, and to reach WT levels at 6 months of age.

In summary, moderate reactive astrogliosis is a feature related to CNS pathology present in MPS VII mouse cortex that could be completely reversed by AAVrh10-GUSB intrathecal administration at the longer treatment time point analyzed.

2.2.6. Behavioral studies

Mice behavior was evaluated by direct observation in the home cage and a battery of tests. Sensorimotor tests evaluated coordination, equilibrium and strength, which can influence the performance in the other tests. Locomotor and exploratory activities were assessed in three different situations: to evaluate neophobia in a new home-cage in the corner test, to estimate the degree of anxiety in an open unprotected space in the open-field test, and to assess spontaneous exploratory behavior in a more protected situation in the T-maze test. Finally, learning and memory were evaluated by a 2-day water maze test.

The data analysis revealed that heterozygote mice displayed a hyperactive behavior when compared to wild type (data not shown). Therefore, HTZ groups were not used as controls in the behavioral analysis and data are not presented.

When comparing 3.5- vs. 6-month-old MPS VII mice, we saw that they scarcely differed in most of the variables measured by the tests (data analysis not shown). At 3.5 months of age, mice already displayed severe MPS VII phenotype, and this behavioral affectation was very similar at 6 months of age. However, we observed a progression of the disease that affected the functional motor capacity of MPS VII mice because it compromised the performance in some tasks.

2.2.6.1. Sensorimotor tests

The sensorimotor tests were performed in order to evaluate equilibrium and coordination, as well as the strength and resistance skills of mice. Sensorimotor data and statistics are reported in **Table 5**.

When coordination was evaluated in the wire rod test, MPS VII mice performed worse than WT, and the AAV treatment was able to improve it at the 6 months time point. Moreover, 3.5-month-old MPS VII mice were worse than WT in the mean distance covered on the 60 s wire hang test. The treatment was able to correct it, since the AAV-treated MPS VII mice values were statistically different from those of the non-treated ones. Regarding strength and prehensility, we observed that MPS VII mice performed worse than WT in the 60 s hang test, displaying lower latency to fall and

using less elements of support. The treatment did not ameliorate these characteristics at any of the time points.

2.2.6.2. Corner test

Corner test was employed to analyze the behavior of the mice related to neophobia. Immediately after placing the mouse in a new environment, its horizontal and vertical activity was recorded during the subsequent 30 seconds. The activity was measured as the number of corners visited and rearings performed. Data and statistics are presented in **Table 5** and **Figure 52**.
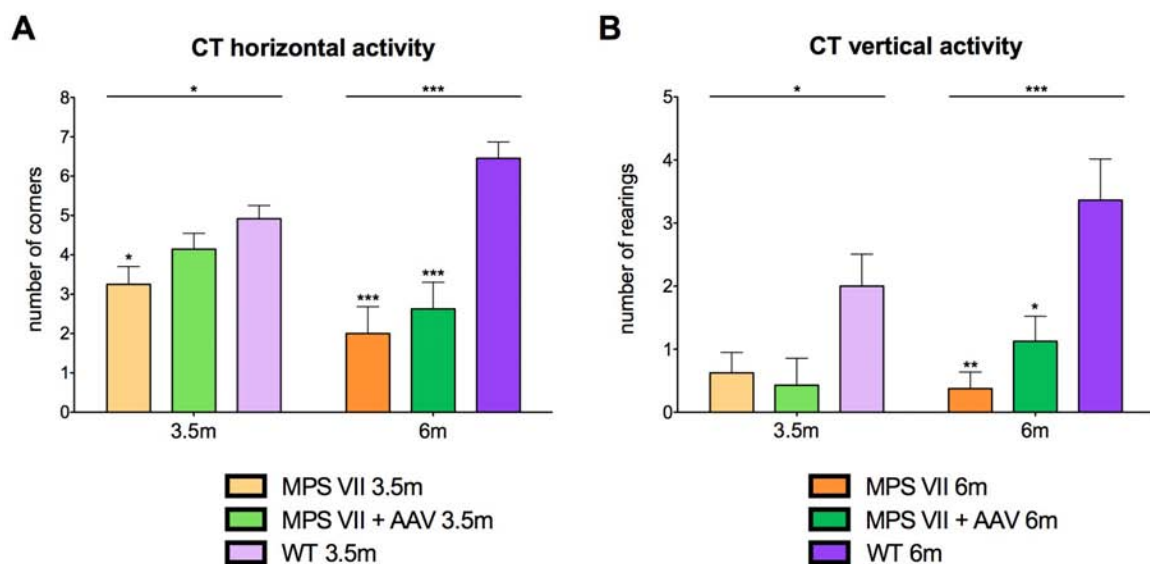
Figure 52: Corner test (CT). (**A**) CT horizontal activity. (**B**) CT vertical activity. Statistics: One-way ANOVA and Tukey *post hoc* for each treatment time point. * vs. WT; # vs. MPS VII. Samples sizes in **Table 5**.

In the corner test, it is shown that MPS VII mice displayed reduced vertical and horizontal activity when compared to WT mice at both ages. The AAV treatment was able to improve the horizontal activity when the short-term schedule was used, but not at long-term, and to slightly increase the vertical activity at long term.

Table 5: Data and statistics of sensorimotor, corner, open field and T-maze tests. Columns show mean ± SEM data and present the statistics of one-way ANOVA and Tukey *post hoc* performed for each time point. * vs. WT; [#] vs. MPS VII. At side, two-way ANOVA for group effect (G), age effect (A), and group per age interaction (GxA). * $p < 0.05$; ** $p < 0.01$; *** $p < 0.001$.

| Table 5. Data and statistics of sensorimotor, corner, open-field and T-maze tests.	3.5m MPS VII (n = 8)	3.5m MPS VII + AAV (n = 7)	3.5m WT (n = 12)	6m MPS VII (n = 8)	6m MPS VII + AAV (n = 8)	6m WT (n = 11)	Two-way ANOVA G	A	GxA
SENSORIMOTOR FUNCTION									
Reflex tests									
Incidence of both reflexes	8/8	7/7	12/12	8/8	8/8	11/11			
Wooden rod test									
Equilibrium (mean latency to fall, s)	20 ± 0	20 ± 0	20 ± 0	20 ± 0	20 ± 0	20 ± 0			
Coordination (mean distance, segments)	0,8 ± 0,4**	1,8 ± 0,7	3,2 ± 0,5	0,9 ± 0,5	1,1 ± 0,6	0,8 ± 0,4		*	*
Wire rod test									
Equilibrium (mean latency to fall, s)	15,1 ± 1	17,2 ± 1,2	15,9 ± 1,4	13,6 ± 2,4	13,7 ± 2,3	14,4 ± 1,8			
Coordination (mean distance, segments)	0,6 ± 0,4**	0,6 ± 0,4**	3 ± 0,5	0,3 ± 0,2*	1,1 ± 0,5	2,1 ± 0,6	***		
Wire hang test (2 trials, 5s)									
Strength (mean latency to fall, s)	3,3 ± 0,6**	4,2 ± 0,3	4,9 ± 0,1	3,5 ± 0,6	2,9 ± 0,6	4,6 ± 0,2	**		
Coordination (mean distance, segments)	0,3 ± 0,1	0,3 ± 0,2	0,5 ± 0,2	0,1 ± 0,1	0,1 ± 0,1	0,3 ± 0,1			
Elements of support (n)	0,4 ± 0,3	0,2 ± 0,2*	1,5 ± 0,3	0,6 ± 0,3	0,3 ± 0,2	0,7 ± 0,3	*		
Wire hang test (1 trial, 60s)									
Strength (mean latency to fall, s)	13 ± 3,9***	24,6 ± 7,3***	58,7 ± 1,3	16,5 ± 6,5***	9,3 ± 3***	54,6 ± 3,8	***		
Coordination (mean distance, segments)	0,5 ± 0,3***	1,3 ± 0,3#	1,9 ± 0,1	0,5 ± 0,3	0,6 ± 0,3	1,4 ± 0,3	***		
Elements of support (n)	0,8 ± 0,4***	0,9 ± 0,6***	2,9 ± 0,1	1 ± 0,4 $^{p=0.053}$	0,4 ± 0,3**	2,2 ± 0,4	***		
CORNER TEST									
Horizontal activity (corners, n) **see Fig. 52A**	3,3 ± 0,5*	4,1 ± 0,4	4,9 ± 0,3	2 ± 0,7***	2,6 ± 0,7***	6,5 ± 0,4	***		**
Vertical activity (rearings, n) **see Fig. 52B**	0,6 ± 0,3	0,4 ± 0,4	2 ± 0,5	0,4 ± 0,3**	1,1 ± 0,4*	3,4 ± 0,7	***		
Vertical activity (latency, s)	26,6 ± 2,4	27,3 ± 2,7	22,6 ± 1,8	26,8 ± 2,1**	21,8 ± 3,6	13,6 ± 2,8	**	*	
OPEN FIELD TEST									
Sequence of events **see Fig. 53A-B**									
Initial movement (latency, s)	2,3 ± 1,2	1,3 ± 0,7	0,4 ± 0,2	1,8 ± 1	0,4 ± 0,4	1,7 ± 0,4			
Exit of the center (latency, s)	11,1 ± 3,2	8,3 ± 2,3	5,1 ± 1,2	45,8 ± 16,5*	7,6 ± 2#	13,8 ± 2,1	**	**	
Entrance to the periphery (latency, s)	39 ± 19,5	23 ± 8,2	19 ± 5,2	63,1 ± 16,7**	17,1 ± 3,9##	17,7 ± 2,2	**		
Vertical activity (latency, s)	126,9 ± 40,5*	83,4 ± 28,8	35,3 ± 10,3	178,1 ± 34,5***	86,3 ± 20#	39,5 ± 4	***		
Vertical activity to wall (latency, s)	149,5 ± 38,2	103,7 ± 32,9	63,1 ± 23,4	206 ± 30,3**	132 ± 29,6	88,6 ± 12,7	**		*
Self-grooming (latency, s)	223,4 ± 34,4	217,6 ± 22	237 ± 20,4	293,1 ± 6,9	233,5 ± 20,4	242,2 ± 21			

Table 5. (Cont.)

	3.5m			6m			Two-way ANOVA		
	MPS VII (n = 8)	MPS VII + AAV (n = 7)	WT (n = 12)	MPS VII (n = 8)	MPS VII + AAV (n = 8)	WT (n = 11)	G	A	GxA
Emotional behavioral events									
Total self-grooming events (n)	1,6 ± 0,8	0,7 ± 0,2	0,7 ± 0,2	0,1 ± 0,1	1,1 ± 0,2##	0,6 ± 0,2			*
Total self-grooming duration (s)	4,6 ± 2,8	3 ± 1,1	2,3 ± 0,7	0,1 ± 0,1*	4,1 ± 0,9#	3,3 ± 1			
Defecation boli (n)	2,3 ± 0,5	1,7 ± 0,6	1,8 ± 0,4	1,5 ± 0,6	1,3 ± 0,3	1,3 ± 0,5			
Urine (1 = presence / 0 = absence)	0,3 ± 0,2	0,3 ± 0,2	0,3 ± 0,1	0 ± 0	0,1 ± 0,1	0,2 ± 0,1			
Horizontal and vertical activities									
Total horizontal activity (crossing n) **see Fig. 53C**	78,6 ± 15,5**	108,4 ± 9,8	142,4 ± 8,6	58,6 ± 11,7***	99 ± 15,2*	159,6 ± 13	***		
Horizontal activity time course **see Fig. 53E and G**							***		
Total vertical activity (rearing n) **see Fig. 53D**	11,1 ± 3,3***	17,9 ± 2,5*	28,6 ± 2,4	6,9 ± 3,7**	17,5 ± 4,8	28,4 ± 2,8	***		
Vertical activity time course **see Fig. 53F and H**							***		
T-MAZE TEST, part 1									
Sequence of events **see Fig. 54B-C**									
Initial movement (latency, s)	53,9 ± 35,3	7,1 ± 1,9	0,6 ± 0,4	5,9 ± 2	8,5 ± 2,1	2,9 ± 2			
Start exploration, turn (latency, s)	59,9 ± 34,4	14,9 ± 3,8	3,5 ± 0,7	28,8 ± 17,7	12,5 ± 3	5,9 ± 2,4	*		
Arrive to maze intersection (latency, s)	115 ± 42,3*	41,6 ± 21,2	11,8 ± 1,7	139,1 ± 43,7*	39,5 ± 15,8#	37,4 ± 9,7	***		
Cross maze intersection (latency, s)	155 ± 44,4**	96,9 ± 38,6	11,8 ± 1,7	171,5 ± 45,2*	112,1 ± 43,3	41,6 ± 9,6	***		
Errors in the long arm (n)	0,3 ± 0,2	0,9 ± 0,4*	0 ± 0	0,1 ± 0,1	0,8 ± 0,3	0,3 ± 0,1	**		
Total errors	0,9 ± 0,6	1,4 ± 0,7	0,6 ± 0,4	0,5 ± 0,3	1,1 ± 0,4	0,5 ± 0,2			
Defecation boli (n)	1,4 ± 0,5	0,3 ± 0,2	0,5 ± 0,2	1,3 ± 0,6	0,4 ± 0,3	0,3 ± 0,2	**		
Urine (1 = presence / 0 = absence)	0 ± 0	0,1 ± 0,1	0,1 ± 0,1	0 ± 0	0,4 ± 0,2	0,1 ± 0,1			
T-MAZE TEST, part 2	(n=5)	(n=5)	(n=12)	(n=5)	(n=5)	(n=11)			
Exploratory efficiency (s) **see Fig. 54D**	119,6 ± 22,9**	115 ± 32,2*	43,3 ± 5,5	158,6 ± 45*	75,4 ± 10,9	66,2 ± 11,1	***		
Mean exploration time, short arms (s)	8,2 ± 1,2	11,9 ± 3,2	9,5 ± 1,6	16,7 ± 3,8	12,3 ± 4,5	8,7 ± 1,4			
Errors in the short arms (n)	1 ± 0,8	0,8 ± 0,4	0,6 ± 0,4	0,6 ± 0,4	0,6 ± 0,2	0,2 ± 0,1			

2.2.6.3. Open-field test

The open-field test records the spontaneous behavior of the mice in a new and exposed environment during 5 minutes. Means and statistics are shown in **Table 5** and **Figure 53**.
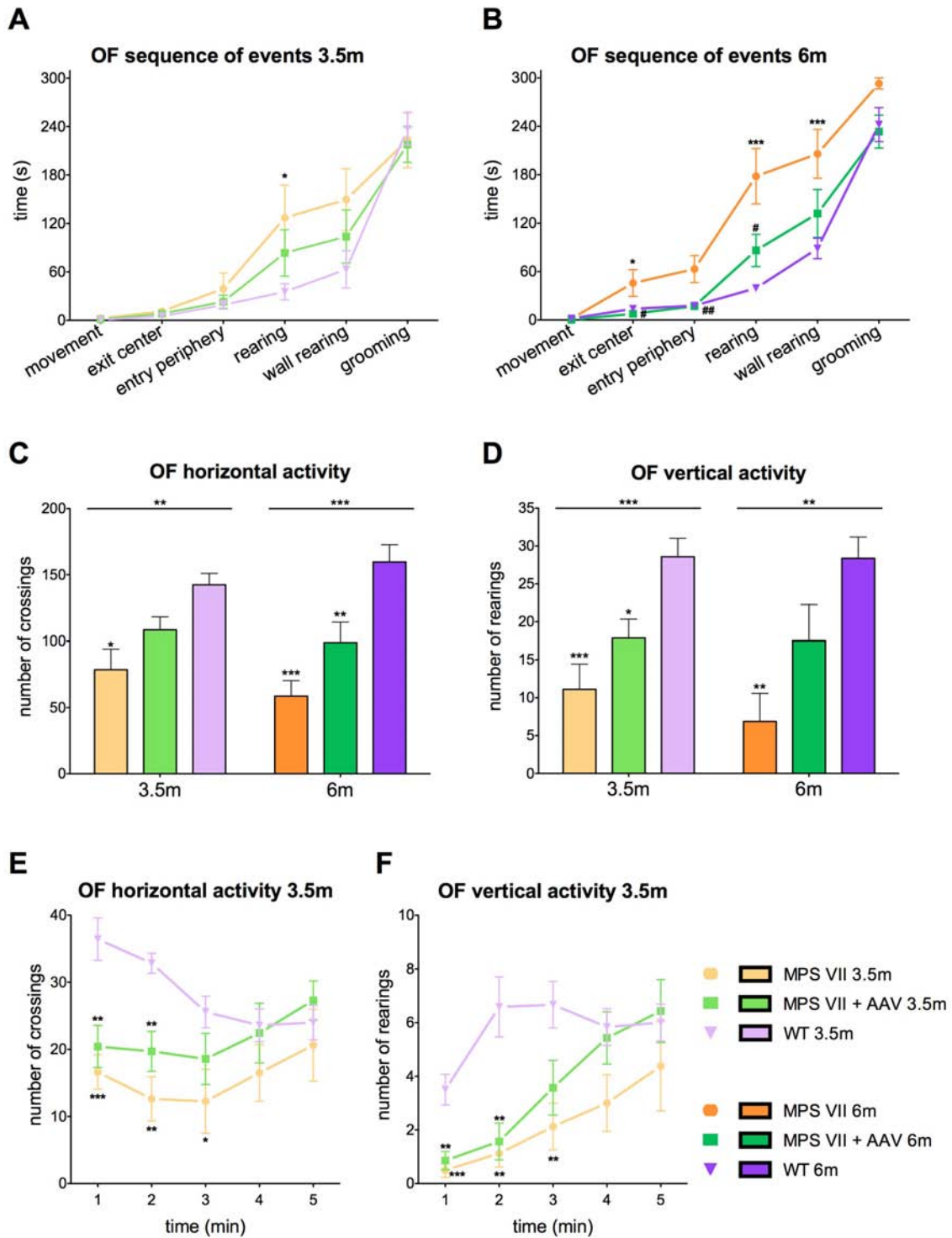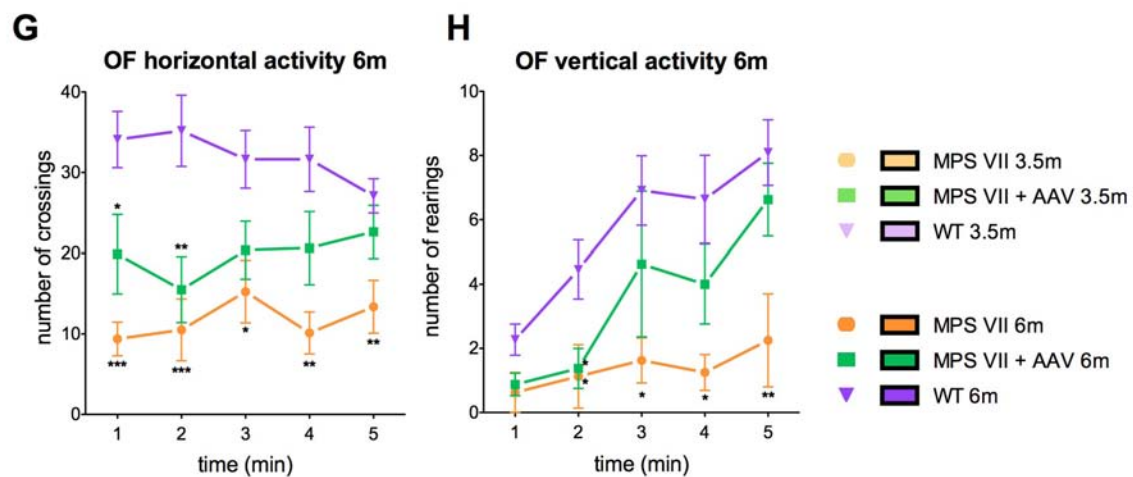
Figure 53: Open field test (OF). (**A**-**B**) OF sequence of events for each time point. (**C**) OF total horizontal activity. (**D**) OF total vertical activity. (**E** and **G**) Time course of OF horizontal activity for each time point. (**F** and **H**) Time course of OF vertical activity for each time point. Statistics: One-way ANOVA and Tukey *post hoc* for each treatment time point: * vs. WT; [#] vs. MPS VII. Samples sizes in Table 6.

Figure 53 A and **B** represent the sequence of behavioral events that take place during the open-field test. It is shown that MPS VII mice developed the sequence of behavioral events slower than WT mice at both ages, being the differences more pronounced at 6 months of age. It is important to notice that data of the grooming activity may present a ceiling effect and, if a longer open-field test was performed, differences among groups in this event could have been detected. In the open-field test, the treatment was capable to significantly improve the sequence of events at long term, as it can be seen with the 6-month-old AAV-treated mice behavior: exit of the center, entry to the periphery and vertical activity were displayed earlier by the AAV-treated than by the non-treated MPS VII mice. Moreover, the total grooming activity of 6-month-old AAV-treated mice was significantly higher than that of the corresponding non-treated group (**Table 5)**

Horizontal and vertical activities in the open-field test are represented in **Figure 53 C** to **H**. MPS VII mice displayed reduced vertical and horizontal activities compared to WT mice. With the AAV treatment, both the horizontal and the vertical activities of MPS VII mice tended to increase respect to the non-treated MPS VII, being the total values statistically significant on the 6-month horizontal activity and on the 3.5-

month vertical activity (**Figure 53 C-D**). When analyzing these activities as a time course throughout the test, the vertical and horizontal activity values of the 3.5-month-old AAV-treated mice were comparable to those of WT mice from the third minute of the test, while the non-treated MPS VII mice were different from WT until the fourth minute of the test (**Figure 53 E-F**). This improvement related to the treatment was more pronounced at 6 months of age, when AAV-treated mice were statistically indistinguishable from WT mice at the third minute of test and up to the end, while MPS VII mice were much less active than WT mice during the whole 5-minute test (**Figure 53 G-H**).

2.2.6.4. T-maze test

T-maze test was performed in order to evaluate the exploratory behavior of mice in a protected environment. The first important thing noticed in the T-maze was that many of the MPS VII mice were not capable to finish the test in 180 seconds. At both experimental time points, in contrast to 100% of the WT mice, only 62.5% of the non-treated MPS VII mice finished the test (**Figure 54A**), which represents a different performance pattern [3.5 months: $\chi^2_{(1,\ n=20)}$ = 5.294, p = 0.021; 6 months: $\chi^2_{(1,\ n=19)}$ = 4.898, p = 0.027]. When MPS VII mice were treated with AAVrh10-GUSB, the proportion of mice that were not able to finish the test was similar to that of the non-treated MPS VII group. Nevertheless, it was qualitatively significant that, at each time point, one AAV-treated mouse was able to explore one of the two short arms of the maze, a fact that was not observed in any of the non-treated MPS VII mice.

Due to the inability of a significant proportion of the MPS VII mice to finish the T-maze task in the established 180 seconds of behavioral recording, the analysis of the data presented in **Table 5** and **Figure 54 B-D**, was done in two parts. First, using the data of all the mice, we analyzed the sequence of events that take place in the long arm of the T-maze, as well as the total number of errors, and defecation and urination. Then, using only the data of the mice that finished the test, we analyzed the exploratory skills. By doing this, we introduced a bias in the data of the MPS VII groups, because we discarded the mice presenting the worst exploratory skills. It is possible that, if the duration of the test had been longer, these mice could have

explored the short arms of the maze and finished the test displaying worse exploratory skills, which would further increase the differences between MPS VII and WT.
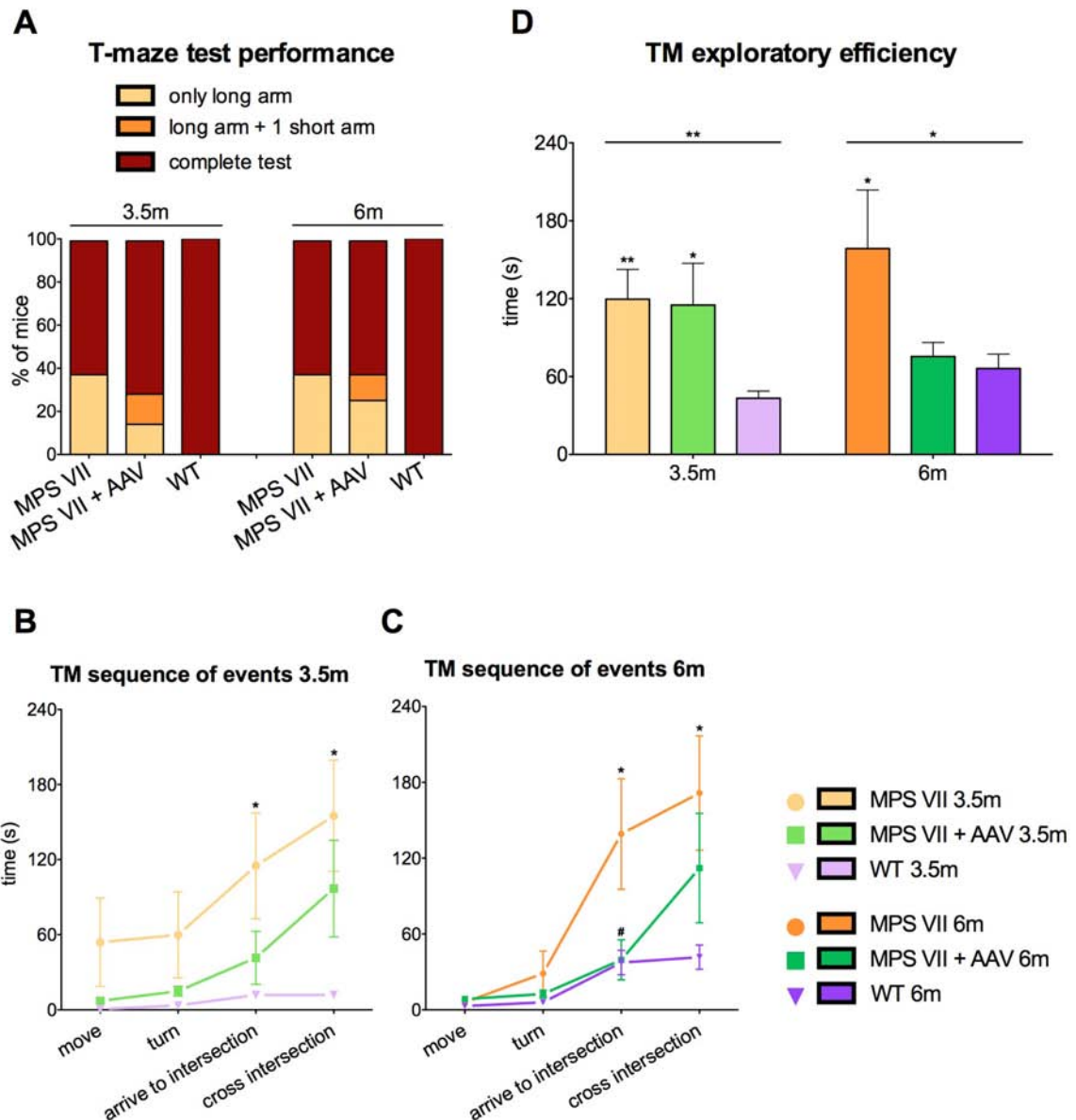

Figure 54: T-maze test (TM). (**A**) Percentage of test completion of the different groups. (**B-C**) Sequence of events in the long arm of the T-maze, at each time point. (**D**) Exploratory efficiency of the mice that finish the test. Statistics in **B**, **C** and **D**: One-way ANOVA and Tukey *post hoc* for each treatment time point. * vs. WT; [#] vs. MPS VII. Samples sizes in Table 6.

The analysis of the sequence of events (**Figure 54 B-C**) revealed that MPS VII latencies to arrive and to cross the maze intersection were longer than those of WT. The AAV treatment improved the performance of MPS VII mice, reducing these latencies to levels that were not distinguishable from WT. Interestingly, 6-month-old AAV-treated MPS VII mice displayed a latency to arrive to the maze intersection statistically different from the non-treated MPS VII mice.

The exploratory skills were assessed after removing the data of the mice that did not complete the test (**Figure 54D**). Results showed that the exploratory efficiency of both treated and non-treated MPS VII mice was higher than WT mice at 3.5 months of age, meaning that both MPS VII groups need more time to complete the test. In contrast, at 6 months of age, only the non-treated MPS VII group was significantly different from WT. This indicated that the treatment with AAVrh10-GUSB was capable to improve the exploratory efficiency of MPS VII mice at long term, but not at short term.

2.2.6.5. 2-Day water maze test

With the aim to evaluate the cognitive function of the MPS VII mice and the effect of the treatment with AAVrh10-GUSB, we performed a 2-day water maze test. This short protocol was chosen to simplify and shorten the tests because MPS VII mice present severe physical deficiencies that difficult their ability to swim. However, even with this short protocol, we could not evaluate the 6-month-old MPS VII mice that did not receive the AAVrh10-GUSB treatment because most of them were not capable to swim properly and there was drowning risk. Interestingly, the MPS VII mice that received the treatment were able to swim and to complete the task in all the cases. Thus, with the water maze test we could demonstrate that the intrathecal treatment with AAVrh10-GUSB was able to correct the motor features of the MPS VII mice to the extent that allowed them to swim properly.

The test consists in two tasks for spatial learning and memory in a water maze. The animals are trained during several consecutive trials (short term memory) to locate the platform and stay there in order to escape from the maze. The two tasks present different levels of difficulty, since the platform is visible on the first day, whereas it is

hidden on the second day. During the trials with the visible platform, mice learn the position of the platform, and the endpoint data are used to establish a baseline for each mouse. On the second day, the trials with the hidden platform assess the cognitive flexibility of the mice because the platform, in addition to being hidden, is located at the opposite side of the pool.

The time that mice need to find the platform and escape from the maze (escape latency) was analyzed, and results are shown in **Figure 55 A** and **D**. Thereafter, swimming distances were measured and mean swimming speed was calculated for each mouse and each trial. The analysis of the swimming speed revealed that 3.5-month-old MPS VII mice were slower than WT (**Figure 55C**). This indicated that the results obtained with the escape latencies were not accurate enough, because the latency depends on the swimming speed. Therefore, the assessment of the learning and memory skills was done by the analysis of the swimming distances (**Figure 55 B** and **E**).
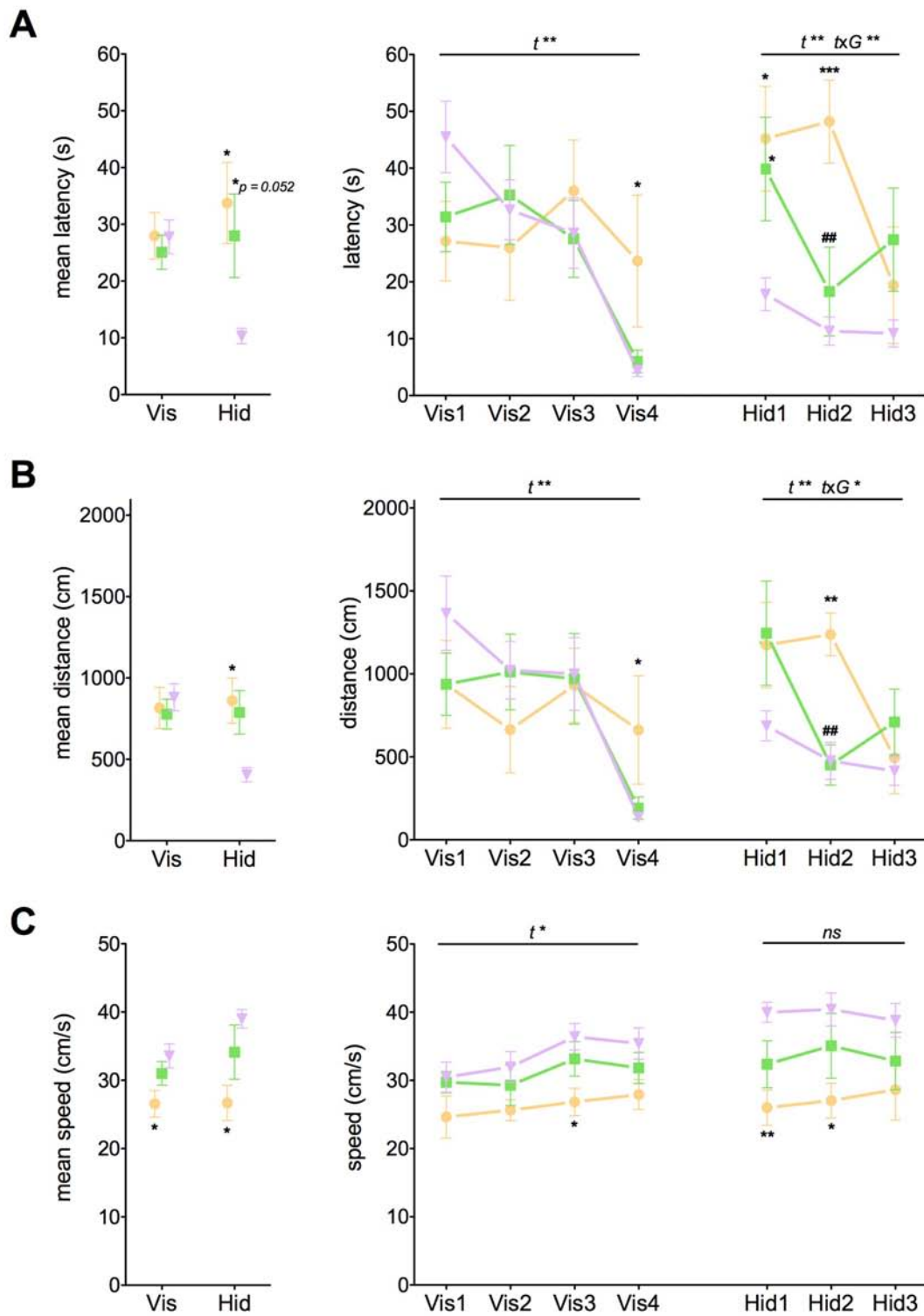
Figure 55: 2-day water maze. (**A** and **D**) Latency to reach the platform (s). (**B** and **E**) Swimming speed (cm/s). (**C** and **F**) Swimming distance to reach the platform (cm). (**A**-**C**) Data of 3.5-month-old mice, mean values at left and "trial by trial" values at right. Statistical analysis by repeated measures ANOVA (RMA), and independent one-way ANOVA for each trial, followed by Tukey *post hoc*.
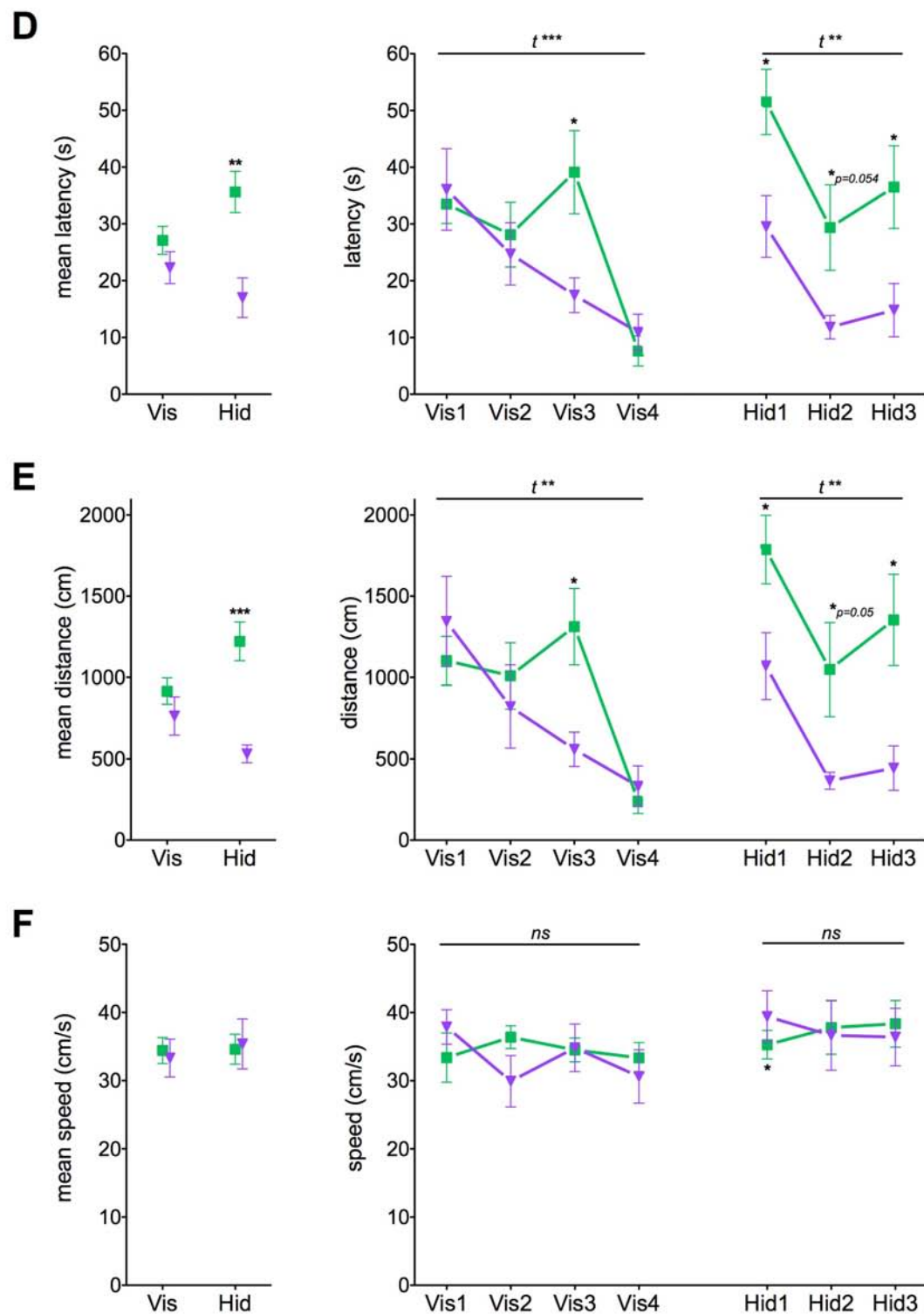
Figure 55 (Cont.): 2-day water maze. (**D**-**F**) Data of 6-month-old mice, mean values at left and "trial by trial" values at right. Statistical analysis performed by RMA, and independent *t*-tests for each trial. *t*, trial effect; *G*, group effect; *txG*, trial per group interaction. * vs. WT; [#] vs. MPS VII. Sample sizes: MPS VII 3.5m, *n* = 5; MPS VII + AAV 3.5m, *n* = 7; WT 3.5m, *n* = 12; MPS VII + AAV 6m, *n* = 8; WT 6m, *n* = 11.

At 3.5 months (**Figure 55B**), the analysis of the mean swimming distance in the visible platform task showed up no difference among groups, with an overall trial effect due to the improvement in the performance of the task throughout the trials. Statistically, there was no differential improvement among groups. However, independent analysis for each trial revealed that MPS VII performed worse than WT in the last trial (*Vis4*) while AAV-treated mice did not. When analyzing the hidden platform task, it was seen that non-treated MPS VII mice covered more distance than WT, while this difference was not statistically significant between AAV-treated MPS VII and WT. The detailed "trial by trial" analysis revealed that the swimming distance decreased throughout the trials with a differential effect depending on the group. Independent analysis of each trial revealed that in the second trial (*Hid2)*, while MPS VII distance was higher than WT, AAV-treated mice displayed values similar to those of WT and statistically different from non-treated MPS VII mice.

At 6 months of age, MPS VII mice could not be tested, and the analysis was done comparing AAV-treated MPS VII mice vs. WT (**Figure 55E**). Mean distance in the visible platform task was not different between WT and AAV-treated mice, while it significantly decreased throughout the trials. This improvement in the performance through the trials was not dependent on the group, although when analyzing each trial by separate, a significant difference in *Vis3* was revealed. In the hidden platform task, mean distance of AAV-treated mice was higher than that of WT. The detailed "trial by trial" analysis showed a trial effect due to the improvement in the performance, which did not depend on the group. Independent analysis of each trial revealed higher swimming distances for AAV-treated MPS VII mice in each trial.

2.2.6.6. Behavioral studies: take-home message

The results obtained in the behavioral analysis of MPS VII mice, and the effect of the treatment with AAVrh10-GUSB on the behavior can be summarized as follows:

Sensorimotor tests revealed that MPS VII mice presented deficiencies in coordination and strength. These are physical deficiencies that compromised the performance in the water maze test: 3.5-month-old mice presented slower swimming speed and 6-month-old mice were not able to swim properly. When assessed in sensorimotor

tests, treatment with AAVrh10-GUSB improved coordination but not strength. Nevertheless, it is important to notice that an overall physical improvement was achieved, which allowed the 6-month-old mice to swim properly. Moreover, both AAV-treated MPS VII groups displayed a swimming speed equivalent to that of WT mice.

In corner test and open-field test, MPS VII mice displayed a less active behavior than WT mice, revealed by lower horizontal and vertical activities in both tests, and a slower sequence of behavioral events in the open-field test. The gene therapy treatment was able to improve the sequence of events and to increase the activity of the MPS VII mice.

In the T-maze test, MPS VII mice showed poorer performance than WT mice: they presented a slower sequence of behavioral events, nearly 40% of MPS VII mice were not capable to complete the test, and those that did it, displayed worse exploratory efficiency than WT. The treatment with AAVrh10-GUSB, although not affecting the percentage of mice that did not complete the test, led to an improvement in the sequence of behavioral events, as well as in exploratory efficiency at long term.

As stated before, a very relevant result was obtained in the 2-day water maze test, where the motor impairment of the 6-month-old MPS VII mice was so severe that they were not able to perform the task, and the treatment restored this capacity. In addition, improvement was achieved concerning learning and memory. In both the visible and hidden platform tasks, 3.5-month-old MPS VII mice presented different learning patterns than WT. In the visible platform task, the treatment improved the patterns so that the baseline achieved in the last trial was exactly the same of the WT. Besides, in the hidden platform task, both MPS VII groups tended to show more difficulties to find the new position of the platform in the first trial. Interestingly, the treatment allowed the MPS VII mice to achieve the levels of performance of the WT already in the second trial, while non-treated mice needed an extra trial to do it. Similar results were obtained at 6 months of age, where it was also seen that the treatment was more efficient in improving an easy task (visible platform) than a difficult task (hidden platform).

Taken together, these results indicate that the intrathecal administration of AAVrh10-GUSB to 8-week-old MPS VII mice leads to an improvement of their behavioral deficiencies.

2.2.7. Survival evaluation

The improvement in the biochemical, histopathological and behavioral characteristics of MPS VII mice after intrathecal treatment with AAVrh10-GUSB led us to analyze whether life expectancy of MPS VII mice would increase with the treatment. Therefore, a group of 20 MPS VII mice were intrathecally injected with AAVrh10-GUSB to evaluate their survival, which was compared to non-treated MPS VII and to heterozygote mice. All mice lived in the animal facility under standard surveillance until they either spontaneously died or were euthanized for ethical reasons due to the poor quality of life. Concerning heterozygote mice, 42% were still alive at the end of the experiment. Results are presented in **Figure 57** and **Table 6**.
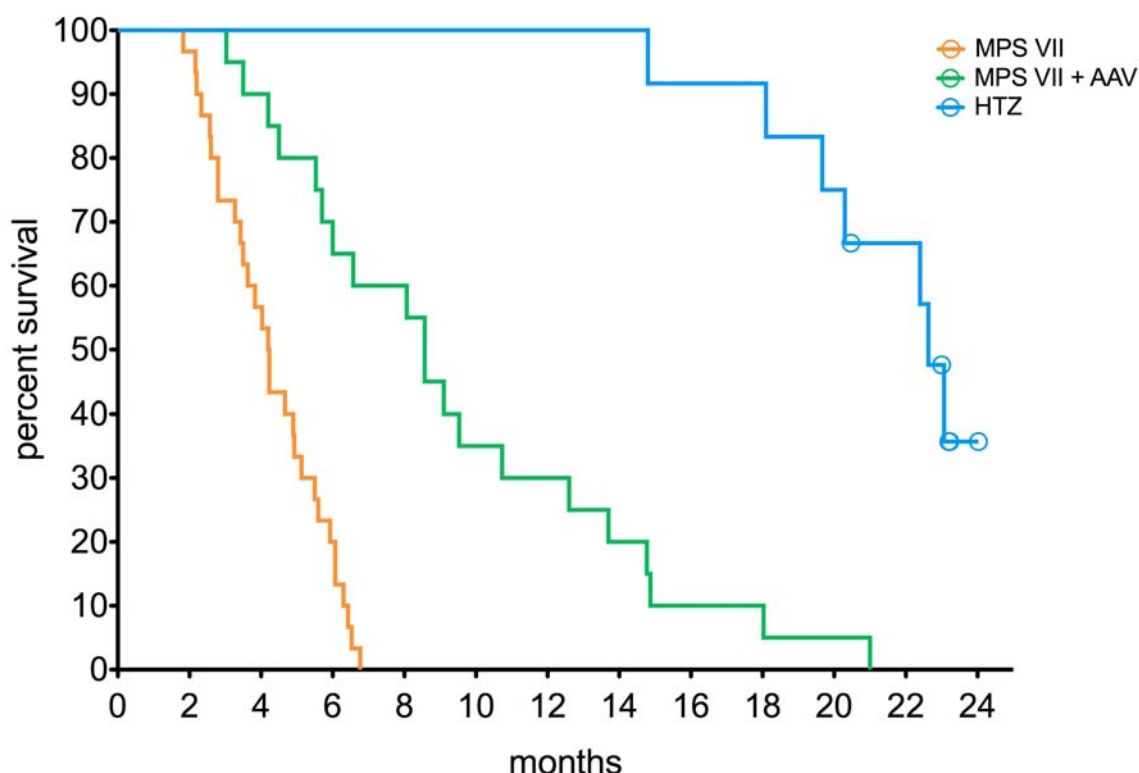

Figure 57: Kaplan-Meier representation of mouse survival. Sample sizes: MPS VII, n = 30; MPS VII + AAV, n = 20; HTZ, n = 12, of which 5 were alive at the end of the experiment, represented with circles. Statistical analysis by Log Rank test: global comparison, p = 10^{-12}; pairwise comparisons, all p < 5×10^{-6}.

Table 6: Descriptive statistics of the survival data.

		sample size	mean ± SEM (months)	median ± SEM (months)
MPS VII	male	13	4.6 ± 0.4	4.9 ± 0.5
	female	17	4.0 ± 0.4	3.8 ± 0.5
	global	30	4.3 ± 0.3	**4.2 ± 0.3**
MPS VII + AAV	male	10	9.3 ± 1.6	8.1 ± 2.0
	female	10	9.5 ± 1.7	8.6 ± 2.2
	global	20	9.4 ± 1.1	**8.6 ± 0.6**
HTZ	male	7 (4)*	21.8 ± 1.2	**
	female	5 (1)*	21.5 ± 0.9	22.6 ± 2.6
	global	12 (5)*	21.7 ± 0.8	**22.6 ± 0.5**
In brackets, number of animals alive at the end of the experiment.				
*** Median for HTZ males could not be calculated because > 50% of individuals were alive at the end of the experiment.*				

MPS VII mice present shortened life span with a median of 4.2 months (126 days), which correlates with previous studies (150 days in Birkenmeier et al. (1991), 154 days in Chen et al. (2012)). **Figure 57** clearly shows that the treatment with AAVrh10-GUSB provides an extension of the life span of MPS VII mice, raising it to a median survival of 8.6 months, which represents 104% increase. Hence, AAVrh10-GUSB, although not restoring normal lifespan, is capable to double MPS VII mice survival, which are very relevant results. Moreover, we determined that the extension of MPS VII life span is independent on the mouse gender, thus being efficient in treating both males and females equivalently (overall and pairwise comparisons between groups by Log Rank test, all *p* > 0.2).

DISCUSSION

DISCUSSION

Mucopolysaccharidosis type VII, searching for a cure

Mucopolysaccharidosis type VII is an autosomal recessive inherited disease affecting less than 1 in 100,000,000 newborns (Orphanet Report Series: prevalence of rare diseases) and presenting high heterogeneity of clinical symptoms. It is an ultrarare disease that is usually manifested in early childhood with severe and progressive symptoms affecting somatic organs, skeletal structures and the nervous system. Life expectancy of MPS VII patients is short; they usually feature a poor quality of life and present mental retardation. Thus, although being a disease with low prevalence, patients present severe affectation that compromises also the quality of life or their relatives. In consequence, it is of interest to find an effective treatment for MPS VII patients. At present, treatments performed to MPS VII patients are directed to ameliorate the symptoms, mainly by surgery, but no curative treatments are currently available. While a lot of research has been conducted in animal models of MPS VII, attempts to provide a curative therapy to MPS VII patients are still scarce.

Mucopolysaccharidosis type VII is caused by a lack of a lysosomal enyme, β-glucuronidase. Research and current treatments available for other mucopolysaccharidoses are based on the rationale of the cross-correction: when lysosomal enzymes are present in the extracellular space, they can be internalized by cell surface receptors and reach the lysosomal compartment. Thus, enzyme replacement therapies provide an exogenous source of enzyme that is internalized by cells, leading to therapeutic benefit. And in hematopoietic stem cell transplant approaches, as well as in gene therapy strategies, cells expressing the lacking enzyme are capable to secrete it to the extracellular medium and provide a source of normal enzyme that can be internalized through the mannose-6-phosphate receptor and provide benefit to neighboring cells.

Following research in animal models and clinical trials in other MPSs, allogeneic hematopoietic stem cell transplant has been attempted in a patient of MPS VII.

Yamada et al. (1998) reported the results of an allogeneic HSCT to a 12-year-old MPS VII female patient that displayed severe locomotor impairment and mental retardation. The treatment achieved amelioration of her motor skills 34 months after transplant while her cognitive abilities remained stable, without improvement. These results, although being good, are only a case report and they cannot be generalized. The benefits of HSCT can considerably vary among patients, depending on many different factors (Prasad and Kurtzberg (2010)), and HSCT is an intervention that presents high biosafety concerns due to transplant rejection.

A strategy that is currently being tested for other diseases affecting CNS is the ex vivo lentiviral gene transfer to hematopoietic progenitors before autologous transplant to the patient. This strategy reported encouraging results in two children affected of X-linked adrenoleukodystrophy (ALD) (Cartier et al. (2009)) and also to three children affected of metachromatic leukodystrophy (MLD), a lysosomal storage disease (Biffi et al. (2013)). Both studies reported that the lentiviral vector integration did not cause genotoxicity. The trial of ALD treated two patients that already displayed CNS affectation and achieved the arrest of the cerebral demyelinating lesions up to 36 months after intervention (Cartier et al. (2012)). The authors claim that these neurological benefits are comparable to those seen in patients undergoing allogeneic HSCT (Cartier and Aubourg (2010)). In the case of MLD, the three patients were diagnosed before the appearance of any clinical symptom because they all had an older sibling affected of MLD. Since MLD is a lysosomal storage disease, the therapeutic protein provided by the transduced cells could be secreted and internalized by adjacent cells leading to cross-correction. Interestingly, they found that the enzyme activity in the CSF of treated patients was comparable to healthy individuals. This treatment achieved the arrest of the progression of the disease in the three patients (Biffi et al. (2013)). Since hematopoietic stem cell transplant is currently the main treatment used for MPS I patients, the results of hematopoietic stem cell gene therapy in metachromatic leukodystrophy could perhaps be translated to this MPS.

However, and despite being HSCT the eligible treatment for some diseases, this intervention still presents a high mortality risk. Even when using HLA-matched

unrelated donor cells, the procedure requires full myeloablation and it raises the mortality risk up to 15 - 20% in children and 30 - 40% in adults (Cartier and Aubourg (2010)). In addition, patients that receive successful HSCT require lifelong immunosuppression and are susceptible to graft-versus-host disease, which are issues that must be taken into account.

In summary, the treatment of MPS VII patients with HSCT presents life-threatening risks and issues that are to be balanced with the expected benefit of the therapy. In this sense, there is no clear evidence that HSCT could provide benefit to patients that are treated when clinical symptoms are already displayed. And unfortunately, most of the MPS VII patients are diagnosed after their symptomatology, when the somatic and/or neurological structures are already impaired.

Following therapeutic approaches used in other MPSs and lysosomal storage diseases, an enzyme replacement therapy clinical trial has been started for MPS VII (*www.clinicaltrials.gov*: NCT01856218) and it is currently ongoing. Recently, Fox et al. (2014) published the first case of a MPS VII patient that received ERT after a compassionate use approval. It is a 12-year-old male patient that presented severe respiratory affectation and required full-time artificial ventilation. He underwent intravenous infusions of recombinant β-glucuronidase every two weeks for 24 weeks. The infusions did not elicit any serious adverse events and achieved a 50% reduction in urinary GAGs. Moreover, the patient showed some improvement in pulmonary function and other life quality items: regained the ability to eat orally, gained weight and increased activity levels. These first results of enzyme replacement for MPS VII are encouraging, since the recombinant protein was well tolerated and led to some therapeutic benefit in the somatic manifestations of the disease. However, we should wait for the clinical trial report to evaluate the safety and efficacy of the treatment, which must be a life-long to provide continued benefit.

Besides, and like in other MPS, intravascular enzyme replacement for MPS VII is not expected to provide any therapeutic benefit to CNS affectation since the recombinant protein cannot cross the blood-brain barrier. In that sense, studies in MPS VII mice revealed that in order to target the CNS it was necessary to start the ERT soon after birth (Vogler et al. (1999)). However, unlike mice, human BBB is completely formed

at birth so neonatal administration of recombinant proteins would not reach the CNS whatsoever.

Vogler et al. (2005) reported in adult MPS VII mice that the administration of large doses of recombinant β-gluc over a sufficient period of time provided therapeutic benefit to the CNS. Besides, different modifications to the β-glucuronidase protein have been tested in mice with the aim to increase the delivery to the brain and bone tissues, with more or less successful results (LeBowitz et al. (2004), (Montaño et al., 2008)). The best results were obtained by Grubb et al. (2008), with a chemical modification on the enzyme that avoids its binding to mannose-6-phosphate receptors and allows its delivery to the cells by alternative unknown receptors. When compared to native β-glucuronidase, the modified enzyme presented lower plasma clearance and higher delivery to brain and bone, achieving improvements in both CNS and skeletal lesions after 12 weeks of weekly injections in MPS VII mice (Huynh et al. (2012), Rowan et al. (2012a)). Some of these modifications on the β-glucuronidase protein, that are still on the animal research field, could also be incorporated to a gene therapy strategy.

As it was said before, the clinical trial of intravenous ERT for MPS VII could provide some therapeutic benefit to MPS VII patients but it is not expected to achieve any CNS benefit. Moerover, the recombinant enzyme infusions are required throughout the patient's life in order to get long-lasting therapeutic effects. In addition, enzyme replacement therapies are some of the most expensive treatments in medicine: ERT for MPS I cost around 300.000 euros per year per patient in 2006 (Beutler (2006)).

In summary, hematopoietic stem cell transplant presents life-threatening risks, and enzyme replacement therapy is a very expensive and life-long treatment that, in addition, cannot provide benefit to the CNS affectation. Therefore, gene therapy appears to be a promising approach for treating mucopolysaccharidosis type VII patients: it can be safer and efficient and performed in one single administration. Thus, vectors that can achieve simultaneous transduction of the CNS and the somatic organs are of great interest.

Intravascular delivery of AAV vectors

It has been described that AAV9 vector, when intravenously delivered to adult mice, it is able to cross the blood-brain barrier and transduce cells in the CNS, besides transducing somatic organs (Foust et al. (2009), Gray et al. (2011)). This feature makes AAV9 a good candidate for intravenous gene delivery to MPS VII mice, a disease affecting both CNS and somatic organs. When this work started, there was not any study about intravenously administered AAVrh10. Therefore, we wanted to check and compare transduction efficiency and tropism of AAV9 and AAVrh10 after IV delivery to adult mice, with the aim to choose the best strategy for MPS VII gene therapy.

Hence, we injected AAV9 and AAVrh10 GFP-expressing vectors via tail vein and checked GFP expression in nervous tissues and liver. In dorsal root ganglia, both serotypes were able to transduce sensory neurons with the same efficiency, while in spinal cord any of them could transduce motor neurons. In contrast, in brain, while we scarcely detected GFP-expressing cells in AAVrh10-injected mice, AAV9-injected mice presented GFP-positive neurons in diverse areas of the brain. In addition, we checked liver transduction as a representative somatic organ that is commonly transduced by gene therapy vectors, and found that both serotypes were able to transduce liver cells, being AAV9 more efficient than AAVrh10 at the same dose. Therefore, in our hands, AAV9 would be a better choice than AAVrh10 for intravenous delivery in order to target both somatic organs and CNS, being able to target neurons in brain. However, does this coincide with previously published articles and with newly published ones?

The works from Foust et al. (2009) and Gray et al. (2011) both describe CNS transduction by IV AAV9 delivery. However, some differences were found in the cell-type specific tropism: while the first described mainly astrocyte transduction, the second found transduction of both neurons and astrocytes. Some works published later on provide more evidence that IV-administered AAV9 is able to transduce neurons, astrocytes, oligodendrocytes and also blood vessels in adult mouse brains and also in spinal cord (Schuster et al. (2014), Yang et al. (2014)). In addition, Yang et al. (2014) also analyzed the outcome of AAVrh10 by intravenous delivery and got

143

very similar results to those of AAV9: efficient and widespread transduction of neurons, astrocytes, oligodendrocytes and blood vessels.

These results do not completely match with our findings. However, differences in experimental procedures could give rise to these incongruences. The vector dose administered (1.93×10^{11} vg in our work vs. 4×10^{12} vg in Yang et al. (2014)), the method of titration of the vector (picogreen vs. qPCR or dot blot) and the mouse strain (ICR mice vs. C57BL/6 mice) could lead to slightly different results in either biodistribution or tropism of the vector. In addition, another difference between our work and the mentioned publications is the detection system of GFP expression: while in this work GFP fluorescence was directly observed, most of the other studies performed immunodetection of GFP. Thus, we could be missing part of the GFP expression that could give rise to higher GFP signal and wider biodistribution (with both AAV9 and AAVrh10). The immunodetection could increase the threshold of GFP detection and highlight cell types other than neurons in the CNS. However, immunolabelling with GFP antibodies could also increase the non-specific background and overestimate the number of transduced cells. Thus, we decided to continue with direct detection of GFP instead of using antibodies against GFP. Finally, we decided to perform intrathecal administration of AAVrh10 vectors to MPS VII mice because we considered that it was safer due to the lower dose required to transduce the CNS. Interestingly, in the last months, transduction of CNS structures after intravenous AAVrh10 administration has also been demonstrated in marmosets (Yang et al. (2014)) and more recently in rats (Hordeaux et al. (2015)).

Another publication that came out after we performed our intravenous experiments is that of Chen et al. (2012) in MPS VII mice. They found that IV administration of AAV9 coding for β-glucuronidase did not provide any therapeutic effect in the CNS of MPS VII mice, while it did so in somatic organs. Surprisingly, in MPS VII mice AAV9 was not able to reach the CNS as efficiently as in normal mice. It had previously been described that sialic acid, a component of the glycan chains of the membrane proteins, could block AAV9 transduction (Shen et al. (2011), Bell et al. (2011)). And Chen et al. (2012) found that MPS VII mice present increased amounts of sialic acid in the brain vasculature that prevent AAV9 transduction. Therefore, after this

144

publication, we can confirm that the intravenous strategy with AAV9 for MPS VII mice was not a good choice.

Intrathecal delivery of AAV vectors

The intrathecal administration through lumbar puncture is currently used in the human clinics to deliver drugs to the central nervous system. It is performed for anesthetic procedures and to administer recombinant enzymes into the CNS for various pathologies. Intrathecal delivery can be performed in an outpatient setting, is much less invasive than intracranial administration, and it and allows access to a wider area of the central nervous system.

Previous results from our group showed that lumbar intrathecal administration of AAVrh10 to adult mice could achieve transduction of sensory neurons in dorsal root ganglia and motor neurons in the spinal cord (Homs et al. (2014)). In the search for a gene therapy strategy for MPS VII, we checked whether this administration route was also able to transduce cells in the brain, and to reach peripheral tissues.

In the CNS, we found out that brains of IT injected mice presented transduction of diverse nuclei and areas of the brain. The AAVrh10-GFP-transduced cells were mainly neurons, and also a few astrocytes and oligodendrocytes. While this work was on progress, Wang et al. (2014) published a similar approach of lumbar intrathecal delivery of AAVrh10 to mice and reported transduction in spinal cord and brain. In addition to AAVrh10, they obtained similar results by intrathecal administration of AAV9. Their results with AAVrh10 correlate with the present work because they also report transduction of neurons, astrocytes and oligodendrocytes. However, while they mention that transduced cells in brain and also in spinal cord were mainly astrocytes, we observed preferential tropism for neurons. Like in our study, they detected direct GFP expression in samples, although they administered half of the dose of AAVrh10 to mice. The differences in the specificity of the tropism could be due to the different vector purification methods used in both works (Klein et al. (2007)).

Besides transducing CNS cells, our work reports that intrathecally injected AAVrh10 was capable to transduce cells of the brain blood vessels in the cortex of C57BL/6 mice, which correlated with strong β-glucuronidase staining in brain blood vessels of AAVrh10-treated MPS VII mice. Surprisingly, we did not observe this feature in ICR mice. And we did not find any publication reporting AAV transduction of brain blood vessels after intra-CSF delivery of AAV vectors. Hence, our work is the first to provide evidence of brain blood vessel transduction after AAV delivery to the CSF. Further studies will be needed in order to characterize which vascular cell types are transduced and to determine the differences among mouse strains.

Some works performing AAV delivery to the CSF reported that transduced cells in brain were clustered around blood vessels after administration of AAV9 to C57BL/6 mice (Schuster et al. (2014)), and AAV9 and AAV7 to NHP (Samaranch et al. (2012), Samaranch et al. (2013)). Following delivery of AAV vectors to the CSF, the entry of the viral particles from the subarachnoid space into the brain parenchyma is likely to happen at the Virchow-Robin space, the paravascular sheath from where CSF and its solutes reach the brain parenchyma (see Figure 6). In this sense, we observed that most of the neuronal nuclei that are transduced after intrathecal AAVrh10 delivery are located close to the paravascular CSF pathways that Iliff et al. (2013) describe as the glymphatic pathway in the rat brain (**Figure 57**). More recently, Hordeaux et al. (2015) reported a patchy transduction pattern around blood vessels after intrathecal delivery of AAVrh10 to adult rats.
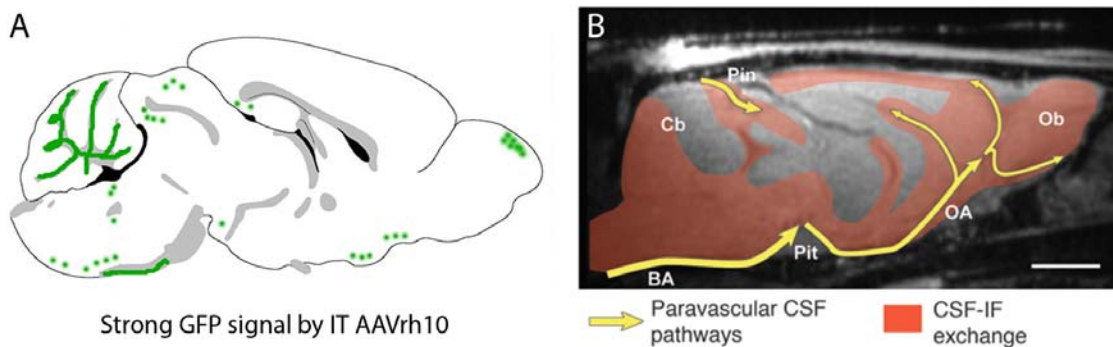

Figure 57: (A) Main brain sites transduced by intrathecal AAVrh10 in the mouse brain. Green dots represent neuronal nuclei while green paths represent axonal tracks. **(B) Paravascular CSF pathways in the rat brain** (yellow arrows) and CSF - interstitial fluid exchange area (orange area) from Iliff et al. (2013). *BA*: basal artery; *Pit*: pituitary recess; *OA*: olfactory artery; *Ob*: olfactory bulb; *Cb*: cerebellum; *Pin*: pineal recess. Scale bar: 3 mm.

Besides CNS transduction, our intrathecal approach using GFP also led to liver transduction by AAVrh10. We analyzed liver as a somatic organ that is commonly targeted by AAV vectors, although other organs such as heart, lung, spleen or kidney could also have been transduced. Liver transduction after intrathecal delivery was an expected feature since some different publications had reported either viral genomes and/or transgene expression in liver after AAV delivery to the CSF in rodents (Towne et al. (2009), Haurigot et al. (2013), Wang et al. (2014), Hordeaux et al. (2015)), dogs (Haurigot et al. (2013)), cats (Hinderer et al. (2014)), pigs (Federici et al. (2012)) and non-human primates (Gray et al. (2013), Samaranch et al. (2012), Samaranch et al. (2013)). Although many evidences of this phenomenon exist, the process by which AAV vectors are drained from the CSF to the blood flow still remains unknown.

Comparison of intravenous and intra-CSF AAV delivery

In this work, the differences observed between intrathecal and intravenous delivery of AAVrh10 concerning CNS and liver transduction are relevant: for IT injection we used a dose nearly 20 times lower than for IV administration (6.5×10^{13} vg/kg for IV vs. 3.3×10^{12} vg/kg for IT), and we obtained better CNS transduction in intrathecal delivery and equivalent liver GFP expression with both administration routes. These results correlate with those of Hordeaux et al. (2015) in rats, who injected a 10-times lower dose of AAVrh10 into de cisterna magna (ICM) than intravenously (2×10^{13} vg/kg for IV vs. 2×10^{12} vg/kg for ICM): they report higher CNS transduction in ICM-injected than in IV-injected rats, while finding equivalent GFP-transduction and vector genomes quantification in liver of both groups.

A similar comparative approach was performed with AAV9 administration in mice (Schuster et al. (2014)) using the same dose of vector for IT and IV delivery. They reported higher CNS transduction performing lumbar intrathecal delivery, and equivalent liver transduction for both administration routes. Besides, another group reported higher brain transduction by ICM delivery of AAV9 than by IV administration, as well as similar transgene expression in liver after both delivery routes, using a 20-times lower dose in the intracisterna administration (Ruzo et al.

(2012), Haurigot et al. (2013)). Therefore, the increased efficiency in liver transduction after CSF delivery may be a common feature of different AAV serotypes.

Taken together, these results show that intra-CSF delivery of AAV9 and AAVrh10 is more efficient than intravenous in targeting CNS and liver. The increased CNS transduction by AAV delivery to CSF is expected, since vectors do not have to cross the blood-brain barrier. However, the higher efficiency in liver transduction by intra-CSF administration than by intravenous AAV delivery is not expected, since AAV vectors can reach the liver easier when directly injected to the bloodstream. It is possible that blood factors could interfere in AAVrh10 liver transduction after intravenous administration, while CSF factors, in contact with the vector prior to its drain to the bloodstream, could somehow protect the AAV and/or enhance its liver transduction capacity. These issues, together with the process that allows AAV vectors to reach the bloodstream after CSF delivery, should be investigated.

When comparing different administration routes to the CSF, both ICM and IT injection are poorly invasive procedures. However, in humans, the cisterna magna is located close to vital centers and the surgery presents high risk of complications. For MPS VII patients, the risk is even higher because they present severe skeletal abnormalities. In contrast, the intrathecal injection is a procedure routinely performed in outpatient settings, thus it also presents less risks for MPS VII patients, which emphasizes the relevance of our choice for the preclinical assay for MPS VII.

Immunogenicity in AAV gene therapy

As it was previously reviewed in this work, preexisting immunity against AAV vectors is an important issue in gene therapy approaches: neutralizing antibodies could preclude transduction of the target organs due to elimination of the vector after delivery.

Different strategies are proposed to overcome the preexisting anti-AAV antibodies in serum and improve the outcome of the gene therapy approach. In gene therapy clinical trials, the selection of the subjects with low or undetectable anti-AAV NAbs allows successful gene transfer, although it would exclude a high proportion of

148

patients. Besides, strategies to decrease the preexisting immunity before AAV administration have also been used. These include plasmapheresis to remove anti-AAV NAbs and transient immunosuppression. These interventions have led to good results but they also present some risks and uncertainties (reviewed by Masat et al. (2013), Calcedo and Wilson (2013), Louis Jeune et al. (2013)).

The administration of very high doses of AAV vector could overcome preexisting anti-AAV NAb levels and allow the transduction of the target tissue. However, the first clinical trial that delivered AAV vectors through the bloodstream revealed that relatively low levels of NAbs could completely neutralize large doses of vector (2 x 10^{12} vg/kg; NAbs 1:17 in Manno et al. (2006)). In addition, the administration of high doses of AAV could trigger a cellular immune response against the capsid and preclude the therapeutic effect. Another way to circumvent preexisting immunity could be engineering the AAV capsids to avoid preexisting serotype-specific NAbs, although the modifications could change the target tissue of the vector and may compromise the vector production titers (reviewed by Bartel et al. (2011)).

In order to avoid neutralization of the AAV vector after injection, the contact of the AAV with NAbs should be minimized. Therefore, when possible, the administration of the AAV vector by delivery routes other than intravascular could potentially improve the outcome of the gene therapy approach.

Concerning CNS-targeted gene therapy strategies, injection of AAV vectors into the brain parenchyma was not expected to be interfered by preexisting anti-AAV immunity in serum, since the levels of NAbs in CSF are much lower than in serum (0.6% NAb CSF/NAb serum; Treleaven et al. (2012)). Early it was demonstrated that very high levels of neutralizing antibodies in serum could decrease and even prevent brain transduction after intracranial AAV delivery (Peden et al. (2004), Sanftner et al. (2004)), However, CNS transduction was unaffected in the presence of lower and clinically relevant NAbs levels in serum (NAb 1:6400, Treleaven et al. (2012)).

When injecting AAV vectors to the cerebrospinal fluid, two different studies in NHP presented different conclusions about NAb interference after AAV9 delivery to the cisterna magna: while Samaranch et al. (2012) found that serum NAb titers higher

than 1:200 could prevent AAV transduction, Gray et al. (2013) reported efficient transduction with NAb titers of 1:128. Supporting the second work, it was reported in dogs that 1:100 to 1:1000 anti-AAV9 NAb titers in serum (reached by preimmunization) allowed efficient CNS transduction after intra-CSF delivery of AAV9 (Haurigot et al. (2013), Ribera et al. (2015)).

What is noteworthy is that the anti-AAV NAb titers that allow CNS transduction by CSF administration would block the transduction if AAV delivery was performed by intravenous injection (Gray et al. (2011), Gray et al. (2013)). Therefore, CSF administration is a better approach than IV to deliver AAV vectors for CNS targeting in order to avoid preexisting immunity. However, AAV vectors administered to the CSF have the ability to reach the bloodstream and transduce somatic organs. Thus, preexisting NAbs in serum, although not affecting CNS transduction, will certainly preclude AAV transduction of somatic organs (Haurigot et al. (2013)), which is necessary to treat diseases like MPSs.

Switching AAV serotypes has also been proposed to overcome the host immunity, because patients may present a different repertoire of anti-AAV NAbs depending on their previous contact with diverse AAV serotypes by natural infections.

Since different AAV serotypes have different capsids and thus display different potential antigens, we expect that different AAV serotypes may induce immune responses that will differ in the specificity of the neutralizing antibodies raised and in the magnitude of the response. Therefore, in designing a gene therapy approach, choosing an AAV serotype that presents low immunogenic response will increase biosafety: preexisting NAbs may be less abundant and the immune response raised by AAV administration would be lower.

In this work, to choose the less immunogenic vector to deliver to MPS VII mice, we studied the immunogenicity raised by AAV9 and AAVrh10 when injected to the mouse bloodstream. We observed that mice injected with AAV9 raised more antibodies than with AAVrh10, which corresponded to greater neutralizing capacity of the serum. These results can be correlated with other works performing intra-CSF delivery of AAV9 in dogs (Haurigot et al. (2013), Ribera et al. (2015)) and of AAVrh10

in non-human primates (Rosenberg et al. (2014)): one week after injection of AAV9 in dogs, serum NAbs raised over 1:1000 with a single dose. In contrast, at the same time after injection, a 4-times lower dose of AAVrh10 in NHP did not raise serum NAbs over 1:120, and those levels decreased to 1:10 at 90 days post-injection. Hence, although using different vector doses and different animal models, the large differences observed in serum NAb after intra-CSF administration could be due to the AAV serotype, thus providing more evidences that AAVrh10 is less immunogenic than AAV9.

Furthermore, since AAVrh10 serotype was isolated from rhesus monkeys, we expected that humans would not have any preexisting immunity against AAVrh10 capsids, thus favoring the choice of AAVrh10 for future hypothetic gene therapy trials in humans. In this sense, a parallel work from our group analyzed the prevalence of AAVrh10 immunogenicity in human serum samples and compared it to AAV9 and AAV2, being the later the most common serotype in humans. The work of Thwaite et al. (2015) describes that AAV9 and AAVrh10 present similar prevalence of anti-AAV antibodies in humans, both being lower than that of AAV2. Moreover, it suggests that this unexpected prevalence of antibodies against a non-human AAV serotype is likely to be caused by cross-recognition of AAV2 specific antibodies. The cross-recognition of antibodies against different AAV serotypes had previously been suggested by Boutin et al. (2010), although AAVrh10 was not included in this study, and it is apparently caused by the high degree of conservation of the aminoacidic sequence of capsid proteins among AAV serotypes. Therefore, the strategy of switching serotypes to circumvent the preexisting immunity may not be effective due to cross-recognition. In addition, when recruiting patients for AAV clinical trials, presence of anti-AAV2 antibodies in their serum could be a cause of exclusion even if this serotype is not to be used in the trial (Thwaite et al. (2015)).

Intrathecal delivery of AAVrh10-GUSB to MPS VII mice

In this work we performed a gene therapy approach to adult MPS VII mice by intrathecal delivery of AAVrh10 coding for β-glucuronidase. This AAV serotype has already been used in a clinical trial for MPS IIIA by intracranial administration

(Tardieu et al. (2014)). Other clinical trials are recruiting patients to perform similar intracranial gene therapy approaches with AAVrh10 for metachromatic leukodystrophy (NCT01801709) and late infantile neuronal ceroid lipofucscinosis (www.clinicaltrials.gov: NCT01161576 and NCT01414985).

Before us, a previous work, published as a brief communication, performed intrathecal delivery of AAV2-GUSB to 5 adult MPS VII mice and achieved lysosomal clearance in brain (Elliger et al. (1999)). However, the vector volume they administered to the CSF was extremely large: they used 100 μl of vector, while the CSF volume of an adult mouse is 35 to 40 μl (Rudick et al. (1982)). Therefore, since they injected three times the total CSF volume, these results are not clinically relevant for the lack of biosafety of the experimental paradigm.

In our pilot study we demonstrated that the intrathecal administration to MPS VII mice of 15 μl containing 5.2×10^{10} vg of AAVrh10-GUSB could achieve transduction of CNS, PNS and liver and lead to high levels of β-glucuronidase activity in these structures and in serum, being in most of the cases much higher than those of heterozygote mice, which do not present lysosomal storage. This enzymatic activity led to a partial or total correction of secondary biochemical alteration, even at very short term. It has been described that overproduction of β-gluc in MPS VII mice (over 20 fold) is not deleterious (Kyle et al. (1990)). However, since previous publications established that 1-5% of wild type β-gluc activity levels were enough to clear lysosomal storage in many tissues (Birkenmeier et al. (1989), Wolfe et al. (1992), Sands et al. (1994)), we decided to decrease the AAV dose in order to increase biosafety.

Thus, after checking that with 1.75×10^{10} vg of AAVrh10-GUSB per mouse (8.75×10^{11} vg/kg) the vector genomes could also be detected in liver, we established this dose for our therapeutic approach, that was administered in 5 μl by intrathecal injection. In order to prevent increased lysosomal storage and cell damage due to disease progression, MPS VII mice were treated when they were young adults, at 8 weeks of age, when mice had grown enough to allow successful manually-guided intrathecal administration. With the aim to check the therapeutic outcome at short and long

term, we established two experimental time points as we did in previous publications of MPS VII mice with a different treatments (Bosch et al. (2000b), Bosch et al. (2000a), Ariza et al. (2014)). We analyzed mice 6 and 16 weeks after AAVrh10-GUSB injection, when mice were 3.5 and 6 months old respectively.

Correction of the nervous system pathology of MPS VII mice

Our intrathecal approach with AAVrh10 achieved widespread β-gluc activity in brain, spinal cord, DRG and sciatic nerve, reaching levels equivalent to those of WT in most of the areas. This widespread distribution was possible because administration to the CSF allows wide distribution of the vector throughout the CNS, and because AAVrh10 can undergo axonal transport and reach distal regions (Cearley and Wolfe (2007)). In addition, β-glucuronidase can also undergo axonal transport and arrive to areas far from the transduction site, as the neuronal axons of the sciatic nerve (Elliger et al. (2002), Passini et al. (2002), Heuer et al. (2002), Berges et al. (2006)).

Correlating with previous published data, lumbar spinal cord and DRG samples presented the highest β-gluc activities due to the proximity to the injection point (Homs et al. (2014)). However, olfactory bulb, the most distal brain area from the injection site, also presented very high β-gluc activity. This fact could be associated to the vector flow through the paravascular CSF pathways, because in the olfactory bulb there is a wide area of exchange between CSF and interstitial fluid (Iliff et al. (2013)). Accordingly, we found in thalamus, basal ganglia and cerebellum the lowest β-gluc activity, which could be related to the areas with less exchange between CSF and interstitial fluid (see Figure 57). The work of Hordeaux et al. (2015) performing ICM injection of AAVrh10 to rats also attributes the observed transduction pattern to the vector distribution by the glymphatic system. Besides, and surprisingly, when administered to the cerebral ventricles (Wang et al. (2014)), AAV9 and AAVrh10 seem to spread in the direction opposite to the CSF flow and give rise to a transduction pattern that also correlates with the paravascular glymphatic system. In addition, correlating to our previous observations with GFP-injected C57BL/6 mice, we observed β-glucuronidase activity in brain blood vessels.

Despite the differences found in β-gluc expression in different brain areas, SC, DRG and sciatic nerve, the biochemical correction in all those areas concerning the secondary β-hex activity elevation was similar: we report a very significant decrease respect to non-treated MPS VII mice in all the areas analyzed. Importantly, since β-gluc activity was sustained from 3.5 to 6 months, this allowed β-hex activity to decrease throughout time. We report that the treatment achieved normalized β-hex activity in half of the different brain areas at 6 months, while reaching nearly normal activity in the other half of the brain and in spinal cord. Therefore, this indicates that long treatment periods are required for better therapeutic outcome.

The assessment of lysosomal function by LAMP-1 protein analysis revealed that MPS VII mice presented increased LAMP-1 expression, which correlates to lysosomal accumulation. However, MPS VII mice also displayed a LAMP-1 expression pattern different from WT mice in all the tissues analyzed: samples presented additional LAMP-1 forms of higher molecular weight, which varied among different tissues. To our knowledge, this feature had not been described in MPS VII or in any other lysosomal storage disease.

LAMP-1 is a glycoprotein presenting large amounts of carbohydrate that contribute to 60% of the total protein mass. Among other saccharides, it presents 18 *N*-linked glycans, some of which are poly-*N*-acetyllactosamines, a high molecular weight glycan present only in a limited number of glycoproteins (Carlsson et al. (1988)). Like for all lysosomal glycoproteins, the glycan chains are bound to the LAMP-1 protein chain in the Golgi complex before they traffic to the lysosome. It has been described that a decreased rate of intracellular transport increases the time that LAMP-1 spends in the Golgi. This fact promotes the binding of an increased number of poly-*N*-acetyllactosamine chains, which also present increased length, thus causing that LAMP-1 displays larger and more heterogeneous molecular weight (Wang et al. (1991)). As for all LSD, it is known that the lysosomal impairment in MPS VII pathogenesis affects cell homeostasis and causes secondary deleterious effects. Among them, the trafficking of lysosomal proteins from the ER to the lysosome compartment could be slowed down. This could cause an increase in the time that LAMP-1 spends in the Golgi complex and the appearance of the larger molecular

weight LAMP-1 forms we observed. In fact, it has been described in the mouse model of MPS IIIB that the vesicular accumulation in neurons is caused by trafficking alterations in the Golgi complex (Vitry et al. (2010)). Further studies of vesicle trafficking in MPS VII mice are required to confirm this hypothesis.

Importantly, we show that in CNS representative areas, AAVrh10 treatment is capable to completely reverse the pathological features of LAMP-1 expression, even at the shortest treatment time point. We observed the decrease in the total amount of LAMP-1 to normal levels, and also the correction of the glycosylation pattern of LAMP-1, possibly caused by the normalization of the Golgi trafficking time.

Taken together, these results show that intrathecal administration of AAVrh10-GUSB to adult MPS VII mice leads to a significant decrease and even a complete reversal of the pathological biochemical hallmarks of the disease.

Interestingly, in brain samples of the different MPS VII treated mice, we observed a correlation between the level of β-gluc activity and subsequent biochemical correction: higher β-gluc activity leads to better correction of β-hex activity and LAMP-1 expression. The different β-gluc expression in brain among different individuals may depend on the magnitude of CNS transduction achieved by the AAV vector, which in turn may depend on the proportion of AAV vector that remains in the CNS vs. the vector that is drained to the blood circulation. In this work we did not find significant correlation between CNS and peripheral β-gluc activity levels, although it could be caused by saturating levels of β-gluc. However, other publications performing intra-CSF delivery of AAV vectors report an inverse relation between CNS and liver transduction (Bevan et al. (2011), Snyder et al. (2011), Federici et al. (2012), Samaranch et al. (2012), Gray et al. (2013), Wang et al. (2014)). Therefore, drainage of the AAV vector to the bloodstream may negatively influence the therapeutic benefit achieved in the CNS, as CSF concentration of the vector is decreased.

The histopathological outcome of the treatment in the nervous system was assessed in cortex and cerebellum, two representative brain areas with high and low β-gluc expression respectively, and in lumbar spinal cord and DRG. Both spinal cord and DRG presented either scarce or no signs of lysosomal accumulation, revealing

correction of the pathology even at the shortest treatment time point. In cortex, treatment achieved complete elimination of vesicle accumulations at both ages. Besides, in cerebellum the AAVrh10-GUSB administration led to 80% correction at 6 months of age, probably due to the lower β-gluc activity achieved in this area. This contrasts with LAMP-1 expression assessment, where we observed complete correction in cerebellum, although it could be due to the lower sensitivity of the western blot technique.

Another pathological feature in the CNS of MPS VII is the moderate reactive astrogliosis, which we assessed in brain cortex. MPS VII mice cortices present reactive astrogliosis that increases from 3.5 to 6 months of age. The intrathecal delivery of AAVrh10-GUSB ameliorates the astrogliosis and can achieve its complete reversal in 6-month-old mice, 4 months after treatment. Therefore, it further demonstrates that long treatment periods are required to achieve correction of pathological hallmarks of MPS VII.

Correction of the somatic pathology of MPS VII mice

The intrathecal gene therapy approach in MPS VII mice achieved sustained levels of β-glucuronidase activity in serum equivalent to those of wild type mice. Our experimental approach ended when mice were 6 months old. However, the longer lifespan of AAV-treated mice −8.6 months median survival of AAV-treated contrasting with 6.8 maximum survival of non-treated MPS VII mice− suggests that β-glucuronidase production and release to the bloodstream is stable over longer periods of time.

Two organs were analyzed as representative of somatic MPS VII pathological features: liver and heart. Mean β-glucuronidase activity in both organs, although presenting high interindividual variability, were comparable to those of WT mice throughout the experiment. Even so, we observed some differences between genders, being male β-gluc activity higher than that of female, in one time point for each organ. This sort of differential transduction between males and females has been reported in liver after intravenous delivery for AAV serotypes 1, 2, 5, 6, 8, and 9 (Davidoff et al.

(2003), Pañeda et al. (2009), Ruzo et al. (2009)) and for AAV9 after delivery to the cisterna magna (Haurigot et al. (2013), Ribera et al. (2015)). This difference in transduction between genders has been attributed to an androgen effect (Davidoff et al. (2003)). In our work, we cannot conclude that AAVrh10 transduction of liver and heart are affected by androgens because the observed differences are not consistent throughout time. Besides, we did not observe any difference between genders in the effect of the treatment in any of the biochemical, histopathological, behavioral or survival parameters analyzed. However, to further address this issue, an experiment with a larger sample size for both genders would be required.

The β-gluc activity detected in liver led to normalization of the biochemical alterations analyzed −β-hexosaminidase activity and LAMP-1 expression− and also achieved clearance of liver lysosomal storage and a complete reversal of hepatomegaly. In heart, although not achieving complete secondary enzymatic correction, LAMP-1 expression was normalized. Despite being one of the organs that are usually refractory to correction, there was no apparent lysosomal storage in cardiac muscle of MPS VII mice after treatment, although we did not analyze cardiac valve morphology.

MPS VII patients present severe skeletal pathological features. In correlation, MPS VII mice also display many skeletal abnormalities: shortened and thickened long bones and malformations in vertebrae and joints, among others (Vogler et al. (1990), Rowan et al. (2012b)). In addition, in MPS VII dogs and patients it has been described that the intervertebral discs present abnormal structure (Smith et al. (2009), Smith et al. (2012a)). Intervertebral disks are the structures that bind two vertebrae together while providing cushioning to the vertebral column, and they are poorly vascularized. Their structure consists in the annulus fibrosus, mainly formed by collagen, that binds the two vertebrae and encloses the nucleus pulposus, a gelatinous substance that contains GAGs (Roberts et al. (2006)). In this work we analyzed the biochemical outcome of AAVrh10-GUSB treatment in lumbar intervertebral discs. Although presenting high interindividual variability among MPS VII treated mice, we could detect mean β-gluc activity levels similar to those of WT mice. This activity led only to a slight decrease in β-hex activity and LAMP-1 expression, but to correction in LAMP-

1 pathologic glycosylation pattern. These results indicate that intrathecal AAVrh10 treatment is able to reach the poorly vascularized intervertebral discs and provide benefit to MPS VII mice. Due to schedule issues, the therapeutic outcome of this treatment on the skeletal abnormalities of MPS VII mice could not be assessed before this manuscript was finished. However, this work is currently ongoing with the radiological analysis of femur and lumbar spine samples by micro-computerized tomography (µCT) and the histopathological assessment of abnormalities in intervertebral discs and knee joints.

Behavioral improvement of MPS VII mice

Behavioral tests are used to assess the physical, emotional and cognitive characteristics of mice. With these tests, species-specific ethograms are defined, which represent the natural behavioral patterns of the species: when animals face a particular situation, their perception and cognition lead to a particular response. Behavioral assessment of MPS VII mice showed up an alteration of the behavioral patterns of mice. The natural responses were attenuated or absent due to the loss of motor, emotional and cognitive abilities. This loss of function compromised the performance in two of the tests: emotional and cognitive deficiencies prevented the completion of the T-maze test, while motor impairment caused the inability to swim in the water maze test. Correlating with this, when MPS VII mice were observed in the home-cage, they displayed less activity and reactivity to the ambient. In this work we demonstrate that the intrathecal injection of AAVrh10-GUSB improves the behavioral pattern of MPS VII mice. The animals that received the treatment displayed responses more similar to those of wild type, with a less attenuated behavior provided by improvements in physical, emotional and cognitive characteristics. In addition, the quantitative improvements led to a very relevant qualitative value: the gain of function in the ability to swim.

Our group previously published a gene therapy approach in MPS VII mice performing an intracranial injection of a canine adenovirus coding for GUSB (Ariza et al. (2014)). β-Glucuronidase activity in CNS provided a similar amelioration of the MPS VII mouse ethogram at short term. However, behavioral analysis of 6-month-old MPS VII mice

could not be performed due to their poor overall physical condition. Hence, the better results achieved by the present work may be attributed to the transduction of somatic organs and the sustained peripheral β-glucuronidase activity.

In our study, the treatment achieved an important behavioral amelioration but it was not able to completely restore the normal mouse ethogram. Nevertheless, this behavioral improvement should be considered a success of the gene therapy approach, taking into account the intrinsic characteristics of behavior and the experimental design.

Behavior depends on a complex neuronal network. By mechanisms that still remain to be elucidated, Mucopolysaccharidosis type VII affects this neuronal network leading to behavioral impairment. In MPS VII mice, this affectation entails a severe phenotype already displayed at early ages and correlated with brain structural abnormalities at later ages (Kumar et al. (2014)). Since MPS VII is caused by the lack of a lysosomal enzyme that is required in all the developmental stages, the disease causes damage to the neuronal network since its formation, which can compromise the behavior from the very beginning. In fact, some studies performing a single behavioral test on 6- or 8-week-old MPS VII mice detected deficiencies in memory and cognition (O'Connor et al. (1998), Sakurai et al. (2004), Fukuhara et al. (2006)).

In this work, mice were treated with the gene therapy vector when they were already 8 weeks old. We did not perform any behavioral characterization of MPS VII mice at this age, but direct observation in the home-cage already revealed lower activity and reactivity to the ambient when compared to wild type mice. Therefore, when the treatment was administered, the neuronal network was already severely damaged or abnormally established due to the disease, and this damage could not be completely reversed by the biochemical restitution. It is possible that an earlier administration of the gene therapy vector could address this issue to some extent, achieving a higher degree of improvement in the MPS VII behavioral pattern. Even so, the aim to completely correct a severe behavioral impairment by a gene therapy strategy should be considered very ambitious. The unknown molecular and physiological mechanisms that lead from the biochemical lack of function to the behavioral MPS VII phenotype may be intricate. Therefore, the mechanisms that lead from the

biochemical correction to the behavioral improvement are neither direct nor easy to extrapolate. They should be addressed in a more direct and specific project, since it is particularly important in sight of future gene therapy clinical trials.

An evidence of this intricate relation between biochemical and behavioral abnormalities is found in heterozygote mice. They present around 50% of the β-glucuronidase activity in the tissues, which is enough to display normal biochemical and histological features. However, heterozygote mice displayed a distinct behavior than that of wild type mice, a more active phenotype. This contrasts with the less active phenotype found in MPS VII mice. This opposite tendency of the behavioral phenotype could be due to compensatory effects of the partial lack of enzymatic function in the heterozygote mice. Further analysis would be required in order to accurately dissect the differences between heterozygote and wild type mice.

Increased survival of MPS VII mice

The improvements achieved in biochemical, histological and behavioral traits of AAV-treated MPS VII mice converge and result in the increase of MPS VII mice life span up to twice the life span of non-treated MPS VII mice, independently of mouse gender. This increase in survival is similar to that achieved by Chen et al. (2012). They developed an AAV2 vector with a capsid modification that targets it to the brain endothelial cells of MPS VII mice specifically (Chen et al. (2009)). When administered intravenously to MPS VII mice (1×10^{12} vg per mouse), this vector was capable to transduce somatic organs and also brain endothelial cells. These cells provided a source of β-gluc that could be internalized by neighboring cells of the CNS, leading to decreased lysosomal storage in many brain areas. Together with our data, this suggests that, to attain increased life span of MPS VII mice, it is not sufficient to achieve correction in peripheral organs but treatments need to specifically target the CNS, a fact that is currently not possible with ERT.

In summary

This work presents a gene therapy approach in adult MPS VII mice based on a single intrathecal injection of AAVrh10 vector coding for β-glucuronidase. This treatment achieves correction of biochemical and histopathological hallmarks of the disease, while providing important improvements in mouse behavioral traits and survival.

The intrathecal administration with a single injection is a poorly invasive delivery route that is routinely performed in human health care, thus an intrathecal gene therapy approach in humans would not present any concerns about the delivery route. The AAVrh10 vector has previously been administered to humans in an intracranial gene therapy clinical trial (Tardieu et al. (2014)) where an immunosuppressive protocol was coadministered to avoid the risk of elimination of transduced cells. In addition, in an intrathecal approach, preexisting immunity may affect AAV transduction efficiency. In our work we provide evidence that AAVrh10 immunogenicity in mice is lower than other serotypes, although the translation to larger animals and humans should take into account the cross-reactivity issues about AAV preexisting immunity.

The treatment is performed with a single injection in the cerebrospinal fluid of adult mice and allows the transduction of CNS and somatic organs, which can only be compared to previous studies performing vector delivery to newborn MPS VII mice. With a single injection, the treatment is capable to attain high β-gluc activity levels in both CNS and somatic tissues, higher than other previously published approaches, and lead to biochemical and histopathological correction. This cellular improvement elicits an important behavioral amelioration and extension of the life span of MPS VII mice. We think that this strategy could achieve even better results if it was performed in newborn mice presenting less affectation due to disease progression. Although it is technically unattainable in mice, it would be more feasible in humans. However, in children, the disease is not usually diagnosed at birth, thus making more difficult the translatability of the treatment to humans. Even so, and corresponding to the literature, the treatment should be administered as early as possible after diagnosis to increase its efficacy.

Future directions

This preclinical assay in mice should be followed by further studies in larger animal models such as the canine MPS VII model. After the description of the dog model of MPS VII (Haskins et al. (1984)) a colony was established and characterized (Haskins et al. (1991)). Since then, some therapeutic strategies have been tested in this canine model.

The first therapeutic approach published in the MPS VII dog was bone marrow transfer, which improved the cardiac pathology (Sammarco et al. (2000)). Later on, and following previous results in mice, the group of K. Ponder published a gene therapy approach in newborn MPS VII dogs by intravenous administration of a retroviral vector coding for GUSB (Xu et al. (2002), Ponder et al. (2002)). They achieved transduction of peripheral organs and β-gluc activity ranging from 1.5 to 60% of WT levels at 6 months. Among all the organs analyzed, liver and spleen displayed the highest β-gluc activity, while brain and muscle the lowest. This led to serum β-gluc levels equivalent to 73% of WT, which were stable for 14 months. This therapeutic approach to newborn MPS VII dogs has further been used and analyzed at longer treatment time points up to 11 years, giving rise to many different publications from the same group. They described that the retroviral vector was able to transduce not only hepatocytes but also blood cells that displayed 5% of WT β-gluc levels and had synergistic therapeutic effects. The neonatal retroviral administration in dogs led to biochemical amelioration and decreased lysosomal storage in many organs, including the brain (Wang et al. (2006)) and bones and joints (Mango et al. (2004)). The treatment improved the MPS VII dog's ability to walk and run, and increased their body weight and survival. The facial morphology was more similar to normal dogs, and some skeletal abnormalities were improved, although not all of them could be prevented (Ponder et al. (2002), Mango et al. (2004), Herati et al. (2008), Smith et al. (2012b), Xing et al. (2013)). In addition, they showed that cardiac abnormalities were also reduced by the retroviral treatment (Ponder et al. (2002), Sleeper et al. (2004), Bigg et al. (2013)). Besides the retroviral therapy, a gene therapy strategy tested in MPS VII dogs is the intracranial injection of a canine adenoviral vector, which was parallel to the results in mice published by our group

(Ariza et al. (2014)). They attained β-gluc expression and correction of lysosomal storage in most of forebrain and midbrain, which was favored by the efficient retrograde transport of the canine adenovirus (Cubizolle et al. (2014)).

The gene therapy strategy proposed in this work should be tested in the canine MPS VII model. Even so, we think that this approach could provide benefit to MPS VII patients compared to current treatments, either available or in clinical trials. This gene therapy treatment would present a lower risk-benefit ratio than hematopoietic stem cell transplant. Besides, contrasting with ERT, a single injection could achieve long term effects and provide therapeutic benefit to CNS affectation. Moreover, this therapeutic approach could also be translated not only to the other types of MPS but also to other LSD.